NASA TECHNICAL NOTE

NASA TN D-8050

NASA TN D-8050

COMPARISON OF TECHNIQUES FOR APPROXIMATING OCEAN BOTTOM TOPOGRAPHY IN A WAVE-REFRACTION COMPUTER MODEL

Lamont R. Poole

Langley Research Center
Hampton, Va. 23665

NATIONAL AERONAUTICS AND SPACE ADMINISTRATION • WASHINGTON, D. C. • NOVEMBER 1975

1. Report No.	2. Government Accession No.	3. Recipient's Catalog No.
NASA TN D-8050		

4. Title and Subtitle	5. Report Date
COMPARISON OF TECHNIQUES FOR APPROXIMATING OCEAN BOTTOM TOPOGRAPHY IN A WAVE-REFRACTION COMPUTER MODEL	November 1975
	6. Performing Organization Code
7. Author(s)	8. Performing Organization Report No.
Lamont R. Poole	L-10320
	10. Work Unit No.
9. Performing Organization Name and Address	161-03-03-01
NASA Langley Research Center Hampton, Va. 23665	11. Contract or Grant No.
	13. Type of Report and Period Covered
12. Sponsoring Agency Name and Address	Technical Note
National Aeronautics and Space Administration Washington, D.C. 20546	14. Sponsoring Agency Code

15. Supplementary Notes

Appendix entitled "Description of Contouring Technique" by James F. Kibler.

16. Abstract

A study of the effects of using different methods for approximating bottom topography in a wave-refraction computer model was conducted. Approximation techniques involving quadratic least squares, cubic least squares, and constrained bicubic polynomial interpolation were compared for computed wave patterns and parameters in the region of Saco Bay, Maine. Although substantial local differences can be attributed to use of the different approximation techniques, results indicated that overall computed wave patterns and parameter distributions were quite similar. More extensive quantitative comparison of computed results with actual wave data would be required in order to select the best approximation technique for refraction studies in which local accuracy in computed results is critical.

17. Key Words (Suggested by Author(s))	18. Distribution Statement
Water waves Wave refraction Numerical approximation	Unclassified – Unlimited Subject Category 48

19. Security Classif. (of this report)	20. Security Classif. (of this page)	21. No. of Pages	22. Price*
Unclassified	Unclassified	44	$3.75

*For sale by the National Technical Information Service, Springfield, Virginia 22161

COMPARISON OF TECHNIQUES FOR APPROXIMATING OCEAN BOTTOM TOPOGRAPHY IN A WAVE-REFRACTION COMPUTER MODEL

Lamont R. Poole
Langley Research Center

SUMMARY

A study of the effects of using different techniques for approximating bottom topography in a wave-refraction computer model was conducted. A mid-Atlantic continental-shelf refraction program was modified to study the region of Saco Bay, Maine. The program employed, on option, topography approximation techniques involving a quadratic least-squares approach, a cubic least-squares approach, or constrained bicubic polynomial interpolation. The results were computed using each of the techniques in conjunction with a given set of initial wave conditions. Comparisons of the results indicated that overall wave-ray and crest patterns were not strongly affected by the choice of approximation technique. The computed crest patterns compared equally well with the pattern observed in vertical aerial photographs of a Saco Bay wavefield. Differences among the comparative patterns in the paths of corresponding individual rays were noted. The path of one particular ray, which was computed using the bicubic polynomial interpolation technique, changed abruptly as the ray passed near an isolated extremum in the input bathymetry data field. Comparative contours at selected levels of wavelength were quite similar; comparative contours at selected wave-height levels, while exhibiting considerable local differences, also showed similarity in overall orientation. For applications in which local accuracy in computed results is critical, more extensive comparison of computed results with actual data on wavelength, direction, and height would be required in order to select the best technique for topography approximation.

INTRODUCTION

In the past, man has made extensive use of the world's coastal regions and adjacent continental-shelf waters for commerce, recreation, and defense purposes. In view of proposals for exploitation of offshore petroleum deposits, construction of offshore power and port facilities, and offshore dumping of sewage sludge and other wastes, the future can only lead to more extensive and complex interactions with the coastal marine environment. Identification of potential safety and pollution problems arising from these

interactions requires improved experimental and analytical techniques for studying the physical phenomena involved.

One such physical phenomenon, a knowledge of which is a most important element in the processes of both offshore and shoreline facility design and site selection, is the behavior of surface waves as they propagate over the continental shelf and impinge on the shoreline. The analytical tool necessary for the study of this process is the wave-refraction model, one such as those models described in references 1 and 2. In the past, such models have been generally limited to small geographical areas such as harbor entrances. Recently, however, the Langley Research Center and the Virginia Institute of Marine Science, in a cooperative effort, have developed a computerized model (ref. 3) for study of wave refraction on the mid-Atlantic continental shelf from Cape Hatteras to Cape Henlopen. A model of this scale (100 n. mi. by 210 n. mi.) is needed in order to identify regional differences in wave behavior to aid in site selection for offshore and shoreline facilities.

The variables of primary influence in an ocean wave-refraction study are the local water depth and its spatial variation. The bottom topography for any large-scale geographic region varies in a generally random fashion. Therefore, the only practical method for the input of bathymetry data to a refraction model is through some type of spatial grid format in which known depth values are supplied at the nodes of the grid. In turn, use of such a grid-type input for bathymetry data necessitates some procedure for determining depth values at intermediate points between nodes and for computing spatial derivatives of the depth for input to other refraction calculations.

Two procedures which have been widely used to approximate bottom topography in refraction computer programs are the quadratic least-squares technique (refs. 1 and 3) and the cubic least-squares technique (ref. 2). Another approximation technique, which has been used by the Coastal Engineering Laboratory of the United States Army Corps of Engineers, involves constrained interpolation with a bicubic (ref. 4, p. 97) polynomial.[1] Each of these techniques is easily applied in a mosaic fashion to large-scale geographic regions. While the constrained bicubic interpolation ensures global continuity in the depth values and certain partial derivatives, the least-squares procedures do not insure continuity in either the depth or its derivatives. Such continuity is desirable from the standpoint of uniqueness in the solution of the refraction equations. On the other hand, the least-squares techniques do provide some smoothing of input bathymetry data (thereby possibly averaging out random error in the data), whereas the constrained bicubic polynomial interpolates through the input data without such smoothing.

---

[1]This interpolation algorithm was obtained through private communication from Dr. D. Lee Harris, Coastal Engineering Research Center, Fort Belvoir, Virginia.

Because of these inherent differences, a study was conducted to investigate the effects on wave-refraction calculations arising from the use of the different techniques to approximate bottom topography. A modified version of the computerized wave-refraction model of reference 3, which employs the quadratic least-squares approximation method, was used in the study. The cubic least-squares and constrained bicubic polynomial approximation techniques were also included in the model. In addition, bathymetry data for the region of Saco Bay, Maine (provided by Dr. Stewart C. Farrell, Stockton State College, Pomona, New Jersey) were substituted for the mid-Atlantic continental-shelf data in the basic model. This small geographic region was selected in order to reference computed wave patterns to vertical aerial photographs of an actual Saco Bay wave pattern (ref. 3, p. 11), as well as to facilitate comparison of overall patterns computed using the different approximation techniques.

A brief discussion is given of the bottom-topography approximation techniques as applied mosaically to a fixed grid system. For a set of initial wave conditions corresponding to those of the Saco Bay wave-pattern photographs, refraction cases were computed using the three approximation techniques under investigation. For these cases, wave-ray and wave-crest patterns, as well as selected contours of equal wave height (constructed using a technique described in the appendix by James F. Kibler) are presented and compared. Selection of the appropriate techniques for bottom-topography approximation in other refraction studies is discussed.

SYMBOLS

$\underline{a}$	vector of constraints for constrained bicubic polynomial interpolation technique
c_{ij}	coefficient of $x^i y^j$ in approximating polynomial
$\underline{c}$	vector of coefficients
d	depth, meters
F	matrix of independent variables evaluated at nodes of 16-node subset in constrained bicubic interpolation technique
H	wave height, meters
h	spacing between nodes in square grid
P(x,y)	bicubic interpolating polynomial

$\mathbf{X}$	matrix of independent variables evaluated at nodes of 12-node subset in least-squares techniques
x	spatial coordinate
y	spatial coordinate orthogonal to x
Z	general function of x and y
ϵ	least-squares approximation error, meters
λ	wavelength, meters

Subscripts:

k	node index in x-direction
ℓ	node index in y-direction
m	local node index in x-direction in 16-node subset
n	local node index in y-direction in 16-node subset
o	initial
p	pth row of $\mathbf{X}$ matrix

A caret (^) denotes an estimate; a prime (′) denotes a transpose of a matrix; and an underlined symbol denotes a vector.

APPROXIMATION OF BOTTOM TOPOGRAPHY

In general, computerized wave-refraction models employ bathymetry data which are supplied in a square-grid format with a fixed individual cell size. Used in conjunction with such a grid system are various techniques for approximating the continuous bottom-topography field to which the discrete bathymetry data apply.

Quadratic Least-Squares Approximation

The model of reference 1 adopted a quadratic least-squares approach for topography approximation within the central cell of a localized 12-node subset of the total bathymetry field. This 12-node subset (see fig. 1) has also been shown to be the near-optimal configuration for use with a two-dimensional quadratic least-squares approximation (ref. 5). The approximating polynomial for the node in the subset located, for example, at coordinates (x_k,y_ℓ) can be written as

$$d_{k,\ell} = \sum_{i=0}^{2} \sum_{j=0}^{2-i} c_{ij} x_k^i y_\ell^j + \epsilon_{k,\ell} \tag{1}$$

where $d_{k,\ell}$ is the actual depth at coordinates (x_k,y_ℓ), c_{ij} are the six coefficients to be determined, and $\epsilon_{k,\ell}$ is the approximation error at the node. For the entire subset, there are 12 linear equations of the form of equation (1) which can be written in matrix form as

$$\underline{d} = X\underline{c} + \underline{\epsilon} \tag{2}$$

where $\underline{d}$, $\underline{c}$, and $\underline{\epsilon}$ are appropriate vectors and X is a matrix whose pth row contains values of the independent variables $\left(x^i y^j\right)$ evaluated at the pth node (p = 1, 2, . . ., 12).

The estimates of the coefficients resulting from application of least-squares principles can be written as

$$\hat{\underline{c}} = (X'X)^{-1}X'\underline{d} \tag{3}$$

where $\hat{\underline{c}}$ is the vector of estimates. Then the depth at any point (x,y) within the central cell of the 12-node subset can be approximated by

$$\hat{d}(x,y) = \sum_{i=0}^{2} \sum_{j=0}^{2-i} \hat{c}_{ij} x^i y^j \tag{4}$$

Partial derivatives of the depth at point (x,y) can be approximated by evaluating analytical partial derivatives of equation (4) at that point.

The matrix X $\left(\text{also } X' \text{ and } (X'X)^{-1}\right)$ in this application contains terms which are functions only of the coordinates of the nodes of the subset of interest. Thus, by using local coordinates (that is, by measuring x and y with respect to some local origin

within the subset) the X matrix (and X', $(X'X)^{-1}$) can be made invariant over the entire region. With reference to equation (3), then, the only new information required for estimating the coefficients for any newly chosen 12-node subset is the vector of actual depths at those nodes. This mosaic least-squares approach can be applied very easily to a large geographical region. This approach also affords some smoothing of the input bathymetry data (which are prone to measurement error and, in reality, are subject to random geological perturbations), but offers no guarantee of continuity in the computed depths or derivatives between cells.

Cubic Least-Squares Approximation

Another technique which can be used for bottom-topography approximation is the cubic least-squares technique such as that employed in the model of reference 2. The approximating polynomial for the node in the bathymetry field located at coordinates (x_k, y_ℓ) can be written in this case as

$$d_{k,\ell} = \sum_{i=0}^{3} \sum_{j=0}^{3-i} c_{ij} x_k^i y_\ell^j + \epsilon_{k,\ell} \tag{5}$$

The model of reference 2 applied such a polynomial to the central cell of the general 12-node subset shown in figure 1. For this subset a set of 12 linear equations of the form of equation (5) can be written similar to equation (2) (with appropriately changed dimensions). Least-squares estimates of the coefficients can be determined by an equation analogous to equation (3) (with 10 estimated coefficients rather than 6, as was the case with the quadratic approach).

The depth at any point (x,y) within the central cell can then be approximated by

$$\hat{d}(x,y) = \sum_{i=0}^{3} \sum_{j=0}^{3-i} \hat{c}_{ij} x^i y^j \tag{6}$$

Again, partial derivatives of the depth at the point (x,y) can be approximated by evaluating analytical partial derivatives of equation (6) at that point.

Again the X, X', and $(X'X)^{-1}$ matrices can be made invariant over the region through the use of local coordinates. Some smoothing of the input bathymetry data results, but to a lesser degree than the smoothing afforded by use of the quadratic least-squares

technique. In using the cubic least-squares method in a mosaic fashion, there again is no guarantee of continuity in computed depths or derivatives between cells.

Constrained Bicubic Polynomial Interpolation

The constrained bicubic polynomial interpolation technique has been used by the Coastal Engineering Laboratory of the U.S. Army Corps of Engineers for bottom-topography approximation. This procedure has the advantage of ensuring continuity in the depth and in certain derivatives of the depth over the entire region under study; its primary disadvantage lies in the fact that it does not provide any smoothing of the input data. However, a separate smoothing algorithm could be used to smooth the raw data prior to the use of the interpolation algorithm.

The general form of the equation representing the approximating surface can be written as

$$P(x,y) = \sum_{i=0}^{3}\sum_{j=0}^{3} c_{ij}x^i y^j \qquad (7)$$

This polynomial is applied to the central cell of the 16-node subset shown in figure 2. The 16 coefficients of the polynomial are determined by applying constraints on the polynomial and on certain of its derivatives at the corner nodes of the central cell. The constraints also insure continuity in the polynomial and constrained derivatives between adjacent cells of interest.

Four constraining conditions are that the value of the polynomial must equal the known depth values at the corner nodes of the central cell, or that

$$P(x_m,y_n) = d_{m,n} \qquad \text{(For all combinations of } m = 2,3;\ n = 2,3) \qquad (8)$$

where m,n are local indices as shown in figure 2.

Eight additional conditions can be stated by constraining the analytical first partial derivatives of equation (7) $\partial P/\partial x$ and $\partial P/\partial y$ at the corner nodes of the central cell to be equal to the central finite-difference approximations of these derivatives. These conditions can be written as

$$\left.\frac{\partial P}{\partial x}\right|_{x=x_m,y=y_n} = \frac{d_{m+1,n} - d_{m-1,n}}{2h} \qquad \text{(For all combinations of } m = 2,3;\ n = 2,3) \qquad (9)$$

and

$$\left.\frac{\partial P}{\partial y}\right|_{x=x_m,y=y_n} = \frac{d_{m,n+1} - d_{m,n-1}}{2h} \quad \text{(For all combinations of } m = 2,3; \; n = 2,3) \tag{10}$$

where h is the distance between adjacent nodal points.

Four additional constraining conditions must be chosen in order to obtain a solution for the 16 polynomial coefficients. One could select from constraints involving any of the three second partial derivatives of the bicubic polynomial. However, constraining the mixed second partial derivative $\partial^2 P/\partial x\, \partial y$ apparently affords some degree of smoothness in both coordinate directions along the approximating surface. Constraining either of the pure second partial derivatives $\partial^2 P/\partial x^2$ or $\partial^2 P/\partial y^2$ would guarantee smoothness in only one direction along the surface. Thus, the four remaining conditions are chosen so as to constrain the analytical mixed second partial derivative of equation (7), that is, $\partial^2 P/\partial x\, \partial y$, to be equal to its finite-difference approximation at the corner nodes of the central cell. These conditions can be written as

$$\left.\frac{\partial^2 P}{\partial x\, \partial y}\right|_{x=x_m,y=y_n} = \frac{d_{m+1,n+1} - d_{m+1,n-1} - d_{m-1,n+1} + d_{m-1,n-1}}{4h^2} \tag{11}$$

(For all combinations of $m = 2,3$; $n = 2,3$)

Conditions in equations (8) to (11), the left-hand sides of which involve forms of the basic polynomial (eq. (7)), thus constitute a set of 16 linear equations in the 16 unknowns $c_{00}, c_{10}, \ldots, c_{23}, c_{33}$. In matrix form, these can be written as

$$F\underline{c} = \underline{a} \tag{12}$$

where F is a 16 X 16 matrix with terms of the form $x^i y^j$ $(i,j = 0,1,2,3)$, $\underline{c}$ is a 16-element vector of the unknown coefficients $c_{00}, c_{10}, \ldots, c_{23}, c_{33}$, and $\underline{a}$ is a 16-element vector the terms of which are the right-hand sides of conditions in equations (8) to (11). The solution to the matrix equation (12) is

$$\underline{c} = F^{-1}\underline{a} \tag{13}$$

The depth and its partial derivatives at any point (x,y) within the central cell can then be approximated by substituting these coefficients into equation (7) and into its appropriate analytical partial derivatives.

For a fixed grid system, the elements of the vector $\underline{a}$ are functions only of input depth values within the 16-node subset and the spacing between nodes. As in the least-squares solutions, if local coordinates are used, the matrix F is invariant as the bicubic interpolating technique is used mosaically over the region of interest. Since the matrix F is invariant over the region, F^{-1} is also invariant and must be computed only once for application to the region under study. Thus, solution for the coefficient vector for any 16-node grouping requires the supply of only the $\underline{a}$ vector, the terms of which again are functions only of input depth values at nodal points of the subset and the spacing between nodes.

COMPARISON OF APPROXIMATION TECHNIQUES

Since the three techniques for bottom-topography approximation discussed in the preceding section differ with regard to input data smoothing and to continuity of the approximating polynomial, quite different results might be expected to arise from the use of the different techniques in similar refraction calculations. In order to assess the magnitude of differences in results, wave patterns and parameters, which are computed by using the different approximation techniques in the same refraction program with a fixed bathymetry data field and a fixed set of initial wave conditions, can be compared.

For the present study, the basic computer routines of the mid-Atlantic continental-shelf wave-refraction program of reference 3 were adopted. As this basic program used only a quadratic least-squares topography approximation technique identical to that of reference 1, options were inserted to allow for the use of the cubic least-squares and bicubic polynomial interpolation techniques. In addition, the bathymetry data field for Saco Bay, Maine, was inserted in a 0.125-nautical-mile square-grid format in the program in place of the basic mid-Atlantic continental-shelf data. The Saco Bay region was selected for the present study for several reasons. The area is sufficiently small in size (9 n. mi. by 7.5 n. mi.) to allow for much easier comparison of overall wave patterns and distributions of parameters such as wavelength and wave height than would be possible for larger regions. At the same time, the complex nature of the Saco Bay bottom topography and shoreline leads to complex wave patterns which are representative of patterns experienced in larger near-coastal regions. A three-dimensional computer-drawn plot of the Saco Bay bathymetry data field (with a vertical exaggeration of approximately 75 to 1) is shown in figure 3. In addition, computed wave patterns can be referenced to an actual wave pattern which was observed in vertical aerial photographs of Saco Bay (fig. 4) and which was used to provide initial conditions and a qualitative verification of the refraction calculations.

RESULTS AND DISCUSSION

In order to compare the topography approximation techniques discussed previously, three cases were computed using the modified mid-Atlantic continental-shelf refraction program with the Saco Bay bathymetry field. From a photogrammetric analysis (ref. 6) of the wave pattern seen in figure 4, the initial wavelength λ_o to be used in each of the cases was determined to be approximately 100 meters; the initial direction of wave propagation was fixed at -135° (with respect to the positive X-axis). By using linear wave theory with an assumption of deep water, the initial wave period was determined from the 100-meter initial wavelength to be 8 seconds. Since the initial wave height could not be determined from the photograph and since it is not a critical parameter with respect to computation of the wave pattern itself, a reference initial height H_o of 1.22 meters was arbitrarily selected.

Wave Patterns

Computed wave-ray (orthogonal to wave crest) patterns for the three cases are presented in figure 5. In a comparison of the three computed patterns, obvious differences in the paths of travel of individual rays can be seen. Of particular interest is the path of ray number 36 in the pattern computed using bicubic interpolation. This ray, which is highlighted in figure 5(c), exhibits an abrupt change in direction at coordinates $x = 15$ grid units and $y = 14$ grid units, near which point (see fig. 3) is located an isolated extremum in the bathymetry data. This abrupt change in direction illustrates the sensitivity of the refraction calculations to isolated extrema (whether real or erroneous) in the bathymetry data. In turn, such extrema in the bathymetry field are emphasized with the use of an interpolative technique such as the present constrained bicubic polynomial technique. This sensitivity suggests that careful verification of real extrema and the removal (such as by presmoothing the data) of erroneous extrema from the data field must be done in order to avoid possibly misleading computations with the use of the constrained bicubic interpolation technique. Neither of the patterns computed using the least-squares theory (figs. 5(a) and 5(b)) exhibits such abrupt changes in ray directions, since the least-squares approach tends automatically to smooth isolated disturbances in the data field.

However, from an overall viewpoint the three patterns show a great deal of similarity. On all three patterns, rays in the number range from 15 to 30 tended to converge and to stop near the island located near $x = 26$, $y = 36$. This tendency is indicative of waves breaking as they approach the island. (See fig. 4.) Similarities also can be noted among the three patterns in the groups of rays which refract around the island, although the group of rays numbered 30 to 40 is less diffuse in the quadratic least-squares pattern (fig. 5(a)) than in either of the other two patterns.

Wave-crest patterns can be derived from computed ray patterns by connecting points which occur at the same time on adjacent rays. The points must be connected in such a manner that the connecting line (crest) is orthogonal to each ray. Accordingly, ray patterns identical to those of figure 5, with the exception of tic marks inserted to denote equal time, were computed. Wave-crest patterns derived from these ray patterns are shown in figure 6. A great deal of similarity can be seen among the three patterns, as could be expected considering the similarities in the ray patterns of figure 5. The most prominent features in the crest patterns are the refraction of crests around the island located near $x = 26$, $y = 36$ and the interaction of two distinct trains of refracted crests in the region near $x = 15$, $y = 25$ to 30. A qualitative examination of the Saco Bay vertical aerial wave photographs (fig. 4) shows similar features in the actual wave pattern.

Contours of Wave Parameters

A more quantitative assessment of the effects of using different bottom-topography approximation techniques in refraction calculations can be made by comparing spatial distributions of computed wave parameters. Two of the more fundamental parameters which can be compared in this manner are the wavelength λ and the wave height H. An effective means for presenting spatial distributions of such parameters is the construction of contours of equal values for the parameter of interest.

Contours of selected values of wavelength and wave height were constructed for the three cases under study by using a technique described in the appendix. The arrays of data points supplied to the contouring program included the wavelength and wave height (and the spatial coordinates) at every odd-numbered data point (in time) along each of the 40 computed rays. Contour curves were then constructed using the cubic spline curve-fitting technique with a tension factor of -3. (See appendix.)

Contours of wavelength for levels of 25, 50, and 75 meters are presented for the three topography approximation techniques in figure 7. Similarities between distinct groups of contours can be noted among the three regional plots. One such group comprises the closed contours for wavelength levels of 75 and 50 meters located near $x = 25$, $y = 36$. Smaller closed contours at the 25-meter level lie interior to these 50- and 75-meter contours on the plots corresponding to the cubic least-squares and constrained bicubic interpolation techniques (figs. 7(b) and 7(c)). These grouped contours are indicative of the reduction in the length of the wave as it approaches and refracts around the island located near these same coordinates. The other distinct group comprises the curved open contours at all three wavelength levels which lie nearer the shore and points out the gradual reduction in the length of the wave as it travels over increasingly shallower water in approaching the shore. As a result of the more constricted local ray pattern (fig. 5(a)) computed using the quadratic least-squares method, the open contours corresponding to the

quadratic least-squares approximation technique (fig. 7(a)) do not approach the X-axis as closely as do those contours corresponding to the other techniques.

The computed wave height is most strongly affected by the relative separation of individual wave rays passing through the local area of interest. (See ref. 7 for details of computation.) For example, as adjacent rays converge, the wave height at points between the two rays tends to increase, and vice versa. Since differences were seen in the paths of corresponding rays in the patterns computed using the different topography approximation techniques, local differences would be expected in comparative wave-height contours. For example, in comparing height contours at the 2.0-meter level for the different techniques (fig. 8), local differences can be noted. However, the contours in the quadratic and cubic least-squares diagrams tend to lie in a pattern oriented in the initial direction of motion of the rays and located on either side of the islands. No such definitive pattern is seen in the bicubic interpolation diagram, although the contours are located seaward and to either side of the island. Similar trends can be noted in the contour diagrams at the 1.5- and 1.0-meter levels which are shown in figures 9 and 10, respectively. However, the pattern in the cubic least-squares diagrams (figs. 9(b) and 10(b)) tends to deviate somewhat from the nominal pattern with the appearance of additional contours shoreward of the island near the center of the general pattern. Comparative contours at the 0.5-meter wave-height level are presented for the three approximation techniques in figure 11. Although great differences can be seen among the three diagrams, the contours are grouped shoreward of the island and, in several areas, are oriented in the same general direction.

Overall Comparison

In an overall manner, the computed wave-ray and wave-crest patterns are not strongly affected by the choice of different topography approximation techniques. Comparative patterns agree equally well in a qualitative manner with vertical aerial photographs of the reference Saco Bay wave pattern from which initial conditions for the comparative cases were drawn. Comparative contours of wavelength and wave height were constructed using computed data along individual wave rays and these contours exhibit similar characteristics in overall contour orientation. However, comparative height contours, in particular, show considerable local differences. In the absence of more quantitative data on the spatial distribution of wavelength and wave height, the best approximation technique cannot be defined; the choice of any of the three techniques could be made with a similar degree of confidence in the resultant overall computed patterns. For those applications in which local accuracy in computed results is critical, more extensive quantitative comparison of computed results with wave-pattern photographs and wave-height data (as might be obtained from use of radar or a laser profilometer) would be required in order to define the best approximation technique.

CONCLUDING REMARKS

A study of the effects of using different techniques for approximating bottom topography in a wave-refraction computer model has been conducted. The basic Langley Research Center – Virginia Institute of Marine Science wave-refraction model was modified to study the region of Saco Bay, Maine, and to include optional topography approximation techniques involving a quadratic least-squares approach, a cubic least-squares approach, or a constrained bicubic polynomial interpolation approach. Comparative refraction cases were run using the three approximation techniques with an assumed initial wave height and fixed initial conditions for wave period and direction derived from vertical aerial photographs of a Saco Bay wave pattern.

Wave-ray and wave-crest patterns computed using the three techniques were quite similar from an overall standpoint, and the crest patterns compared well, in a qualitative sense, with the reference photographs. However, some differences were noted in the paths of corresponding rays in the comparative patterns. The path of one particular ray, which was computed using the constrained bicubic interpolation technique, exhibited an abrupt change in direction in the vicinity of an isolated extremum in the bathymetry data field. This change in direction illustrates the sensitivity of refraction calculations to such an extremum (whether real or erroneous) the importance of which, in turn, is emphasized with the use of an interpolation technique such as the present constrained bicubic polynomial. This sensitivity implies that verification of real extrema and removal of erroneous extrema in the data field are required in order to avoid possibly misleading computations with the use of the bicubic interpolation technique. Contours were constructed at selected levels of wavelength and wave height for the three comparative cases. Comparative wavelength contours were quite similar, and even though considerable differences could be observed in local areas in the comparative wave-height contour diagrams, a similar pattern of orientation on a gross scale could be noted.

In light of the absence of actual wave-height data for comparison, the best approximation technique could not be defined, and any of the three techniques could be expected to yield comparable overall results. For applications in which local accuracy in computed results is critical, more extensive quantitative comparison of computed results with actual wave data would be necessary in order to determine the proper topography approximation technique.

Langley Research Center
National Aeronautics and Space Administration
Hampton, Va. 23665
August 14, 1975

APPENDIX

DESCRIPTION OF CONTOURING TECHNIQUE

James F. Kibler
Langley Research Center

A contour plot is a convenient way to display a function of two independent variables. The contour is simply a line connecting constant values of the function plotted on a grid composed of the corresponding independent variables. In this way, a three-dimensional surface can be easily visualized in two dimensions. The purpose of this appendix is to describe briefly the contouring technique used to generate the contour plots of wavelength and wave height presented in this paper. The technique was developed by C. L. Lawson of the Jet Propulsion Laboratory and modified by A. K. Cline of the Institute for Computer Applications in Science and Engineering at the Langley Research Center.

Assume that the function to be contoured is available as an array of randomly spaced data points. Each data point consists of an x, y, and Z value. The x and y values correspond to the independent coordinates to be plotted and $Z = Z(x,y)$ is the function value to be contoured. The contouring process begins by forming a convex region composed of triangles from the set of x-y data points (fig. 12). Figure 12(b) illustrates an arrangement of triangles which form a convex region from the data points in figure 12(a). Obviously, this arrangement is not unique. A somewhat arbitrary criterion is established to maximize the smallest interior angle between possible pairs of triangles. For example, with a set of four data points there are two choices for arranging the two triangles (fig. 13). Under the above criterion, figure 13(b) is chosen as the preferred arrangement. That is, the smallest interior angle in figure 13(b) is larger than the smallest interior angle in figure 13(a).

After the triangles are arranged, each Z value is assigned to its corresponding x-y vertex in each triangle. An interpolating plane which fits the vertices exactly is then calculated for each triangle. If a chosen contour level lies between the Z values for any triangle, the two contour points which lie on the sides of the triangle are computed from the interpolating plane (fig. 14). These contour points are calculated for each triangle in the convex region and for each specified contour level. The contour points for any given contour level may then be connected by straight lines to yield a polygonal approximation to the required contour. Alternatively, a method involving a cubic spline function under tension can be used to fit a smooth curve to each set of contour points. (For example, see ref. 8.) This curve fits the interpolated contour points exactly and

varies smoothly between them. The tension factor may be adjusted to yield suitable curves. (A large factor corresponds to straight lines between contour points.)

The contours which result from this technique are only approximate. Their accuracy is limited by the linear interpolating procedure and is dependent upon the density of the available data.

REFERENCES

1. Dobson, R. S.: Some Applications of a Digital Computer to Hydraulic Engineering Problems. Tech. Rep. No. 80 (Contract Nonr 225(85)), Dep. Civil Eng., Stanford Univ., June 1967. (Available from DDC as AD 659 309.)
2. Mehr, Emanuel: Surf Refraction – Computer Refraction Program. NWRF 36-0962-068, U.S. Navy, Sept. 1962.
3. Goldsmith, Victor; Morris, W. Douglas; Byrne, Robert J.; and Whitlock, Charles H.: Wave Climate Model of the Mid-Atlantic Shelf and Shoreline (Virginia Sea) – Model Development, Shelf Geomorphology, and Preliminary Results. NASA SP-358 (VIMS SRAMSOE No. 38), 1974.
4. Hayes, J. G.: Fitting Data in More Than One Variable. Numerical Approximation to Functions and Data, J. G. Hayes, ed., Athlone Press (London), 1970, pp. 84-97.
5. Canavos, George C.: Criteria for the Optimal Design of Experimental Tests. NASA TM X-2663, 1972.
6. Farrell, Stewart C.: Present Coastal Processes, Recorded Changes, and the Post-Pleistocene Geologic Record of Saco Bay, Maine. Ph. D. Thesis, Univ. of Massachusetts, 1972.
7. Munk, W. H.; and Arthur, R. S.: Wave Intensity Along a Refracted Ray. NBS Circ. 521, U.S. Dep. of Commerce, 1952, pp. 95-108.
8. Schweikert, Daniel G.: An Interpolation Curve Using a Spline in Tension. J. Math. & Phys., vol. XLV, no. 3, Sept. 1966, pp. 312-317.

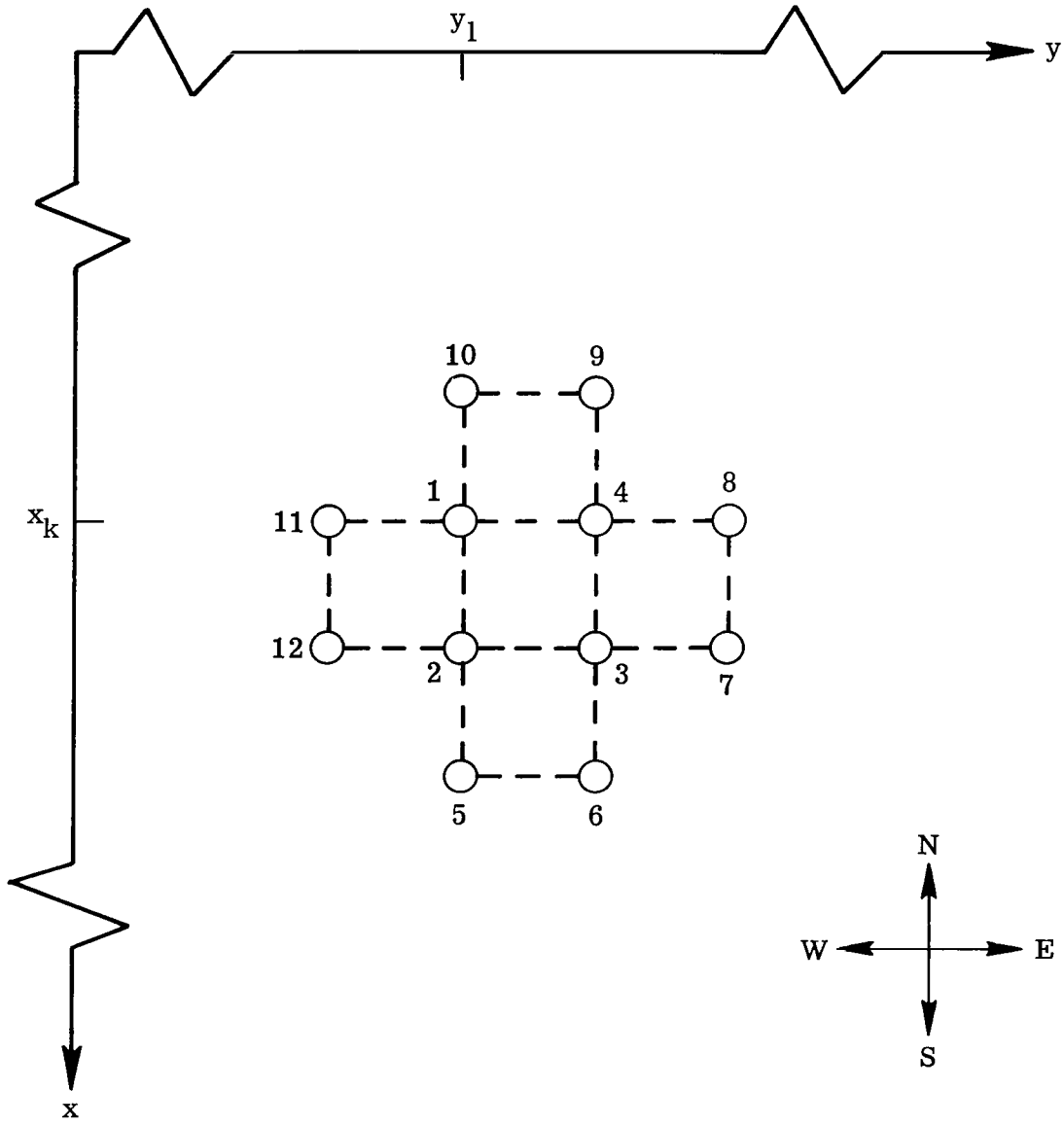

Figure 1.- Twelve-node subset of bathymetry data field to which quadratic and cubic least-squares approximations are applied.

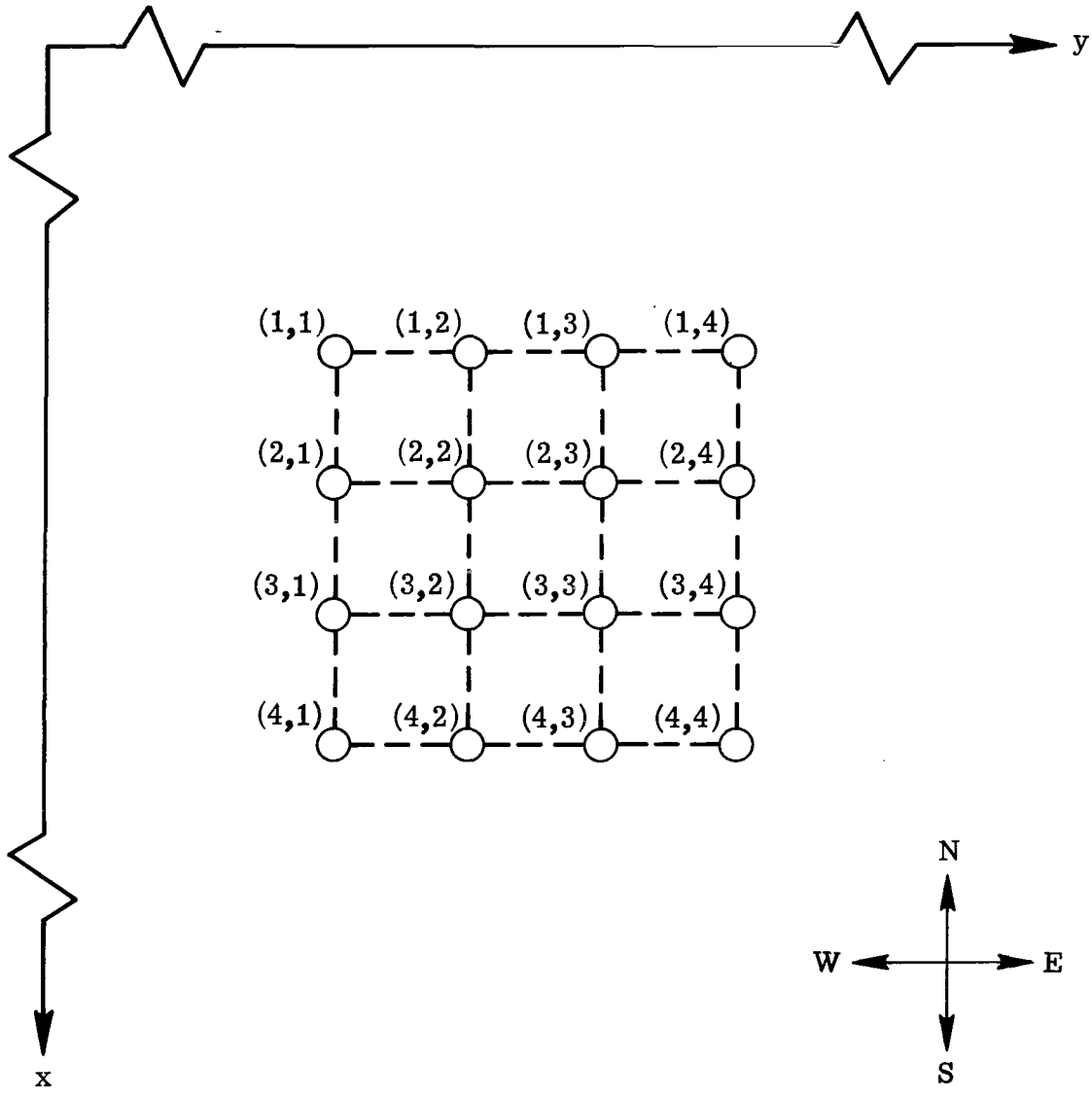

Figure 2.- Sixteen-node subset of bathymetry data field to which constrained bicubic polynomial interpolation is applied.

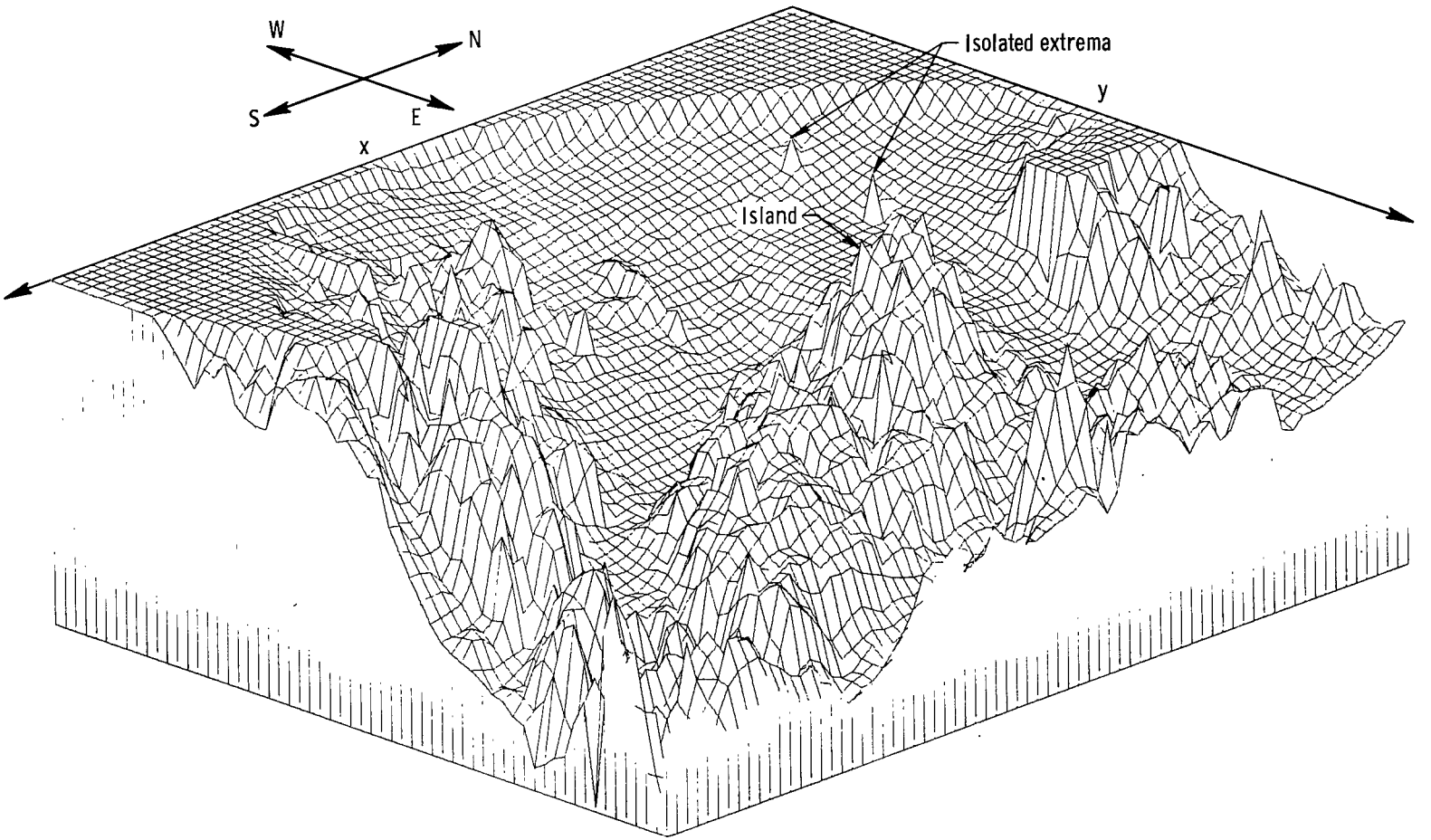

Figure 3.- Three-dimensional computer-drawn plot of bathymetry data field for Saco Bay, Maine. Vertical exaggeration, 75 to 1.

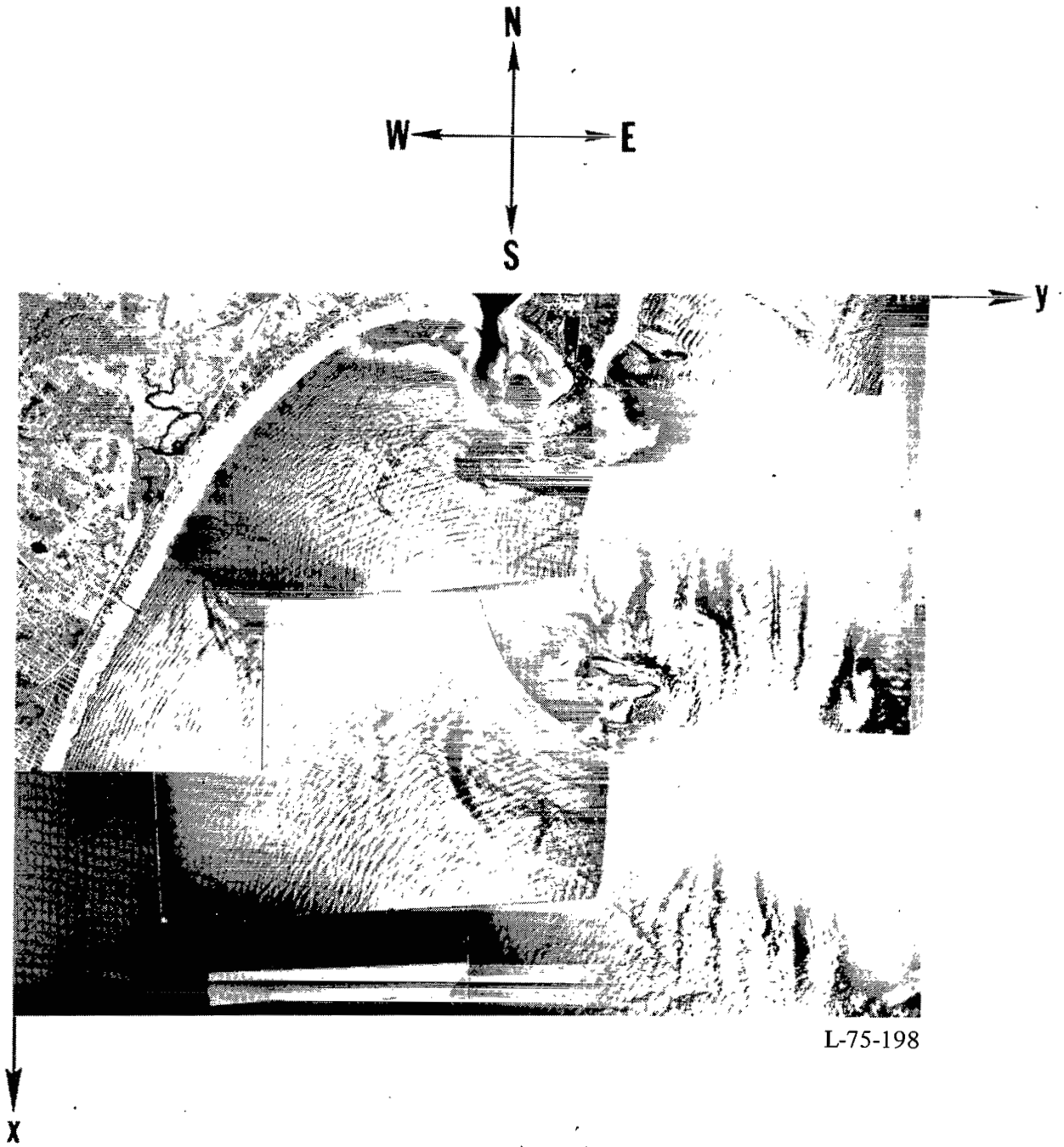

Figure 4.- Mosaic of vertical aerial photographs of a Saco Bay, Maine, wave pattern (from ref. 3).

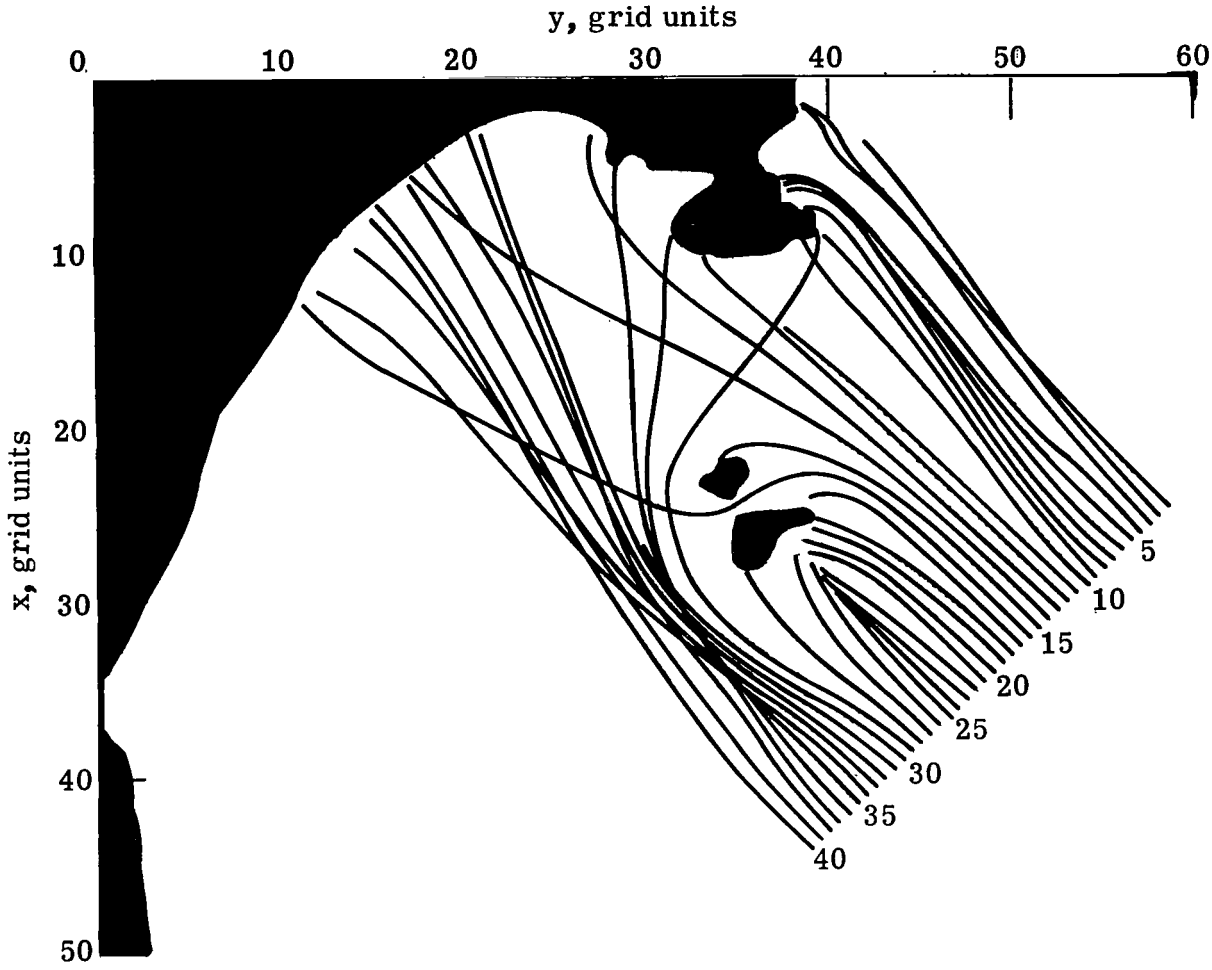

(a) Quadratic least squares.

Figure 5.- Saco Bay wave-ray patterns computed by using different topography approximation techniques.

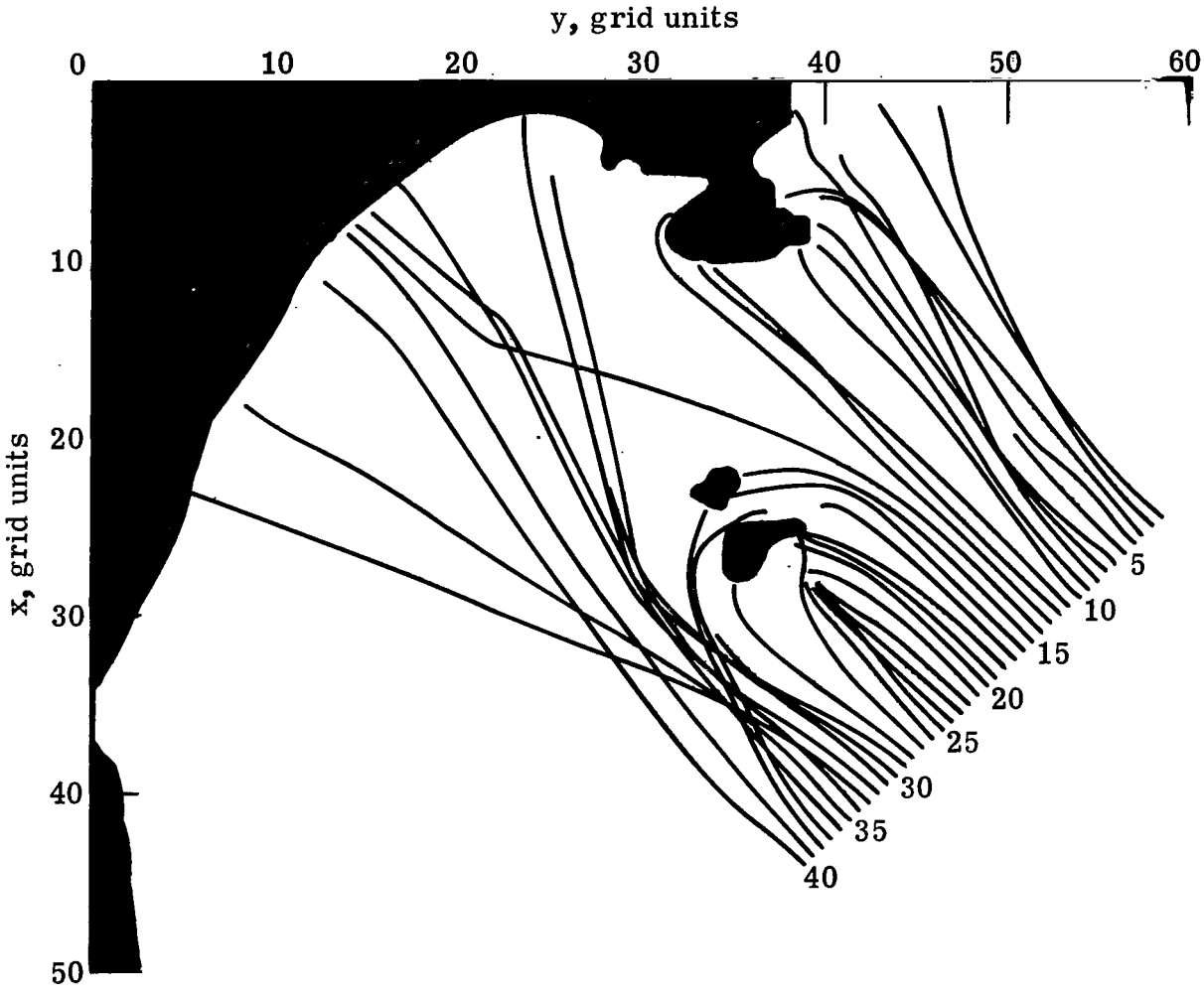

(b) Cubic least squares.

Figure 5.- Continued.

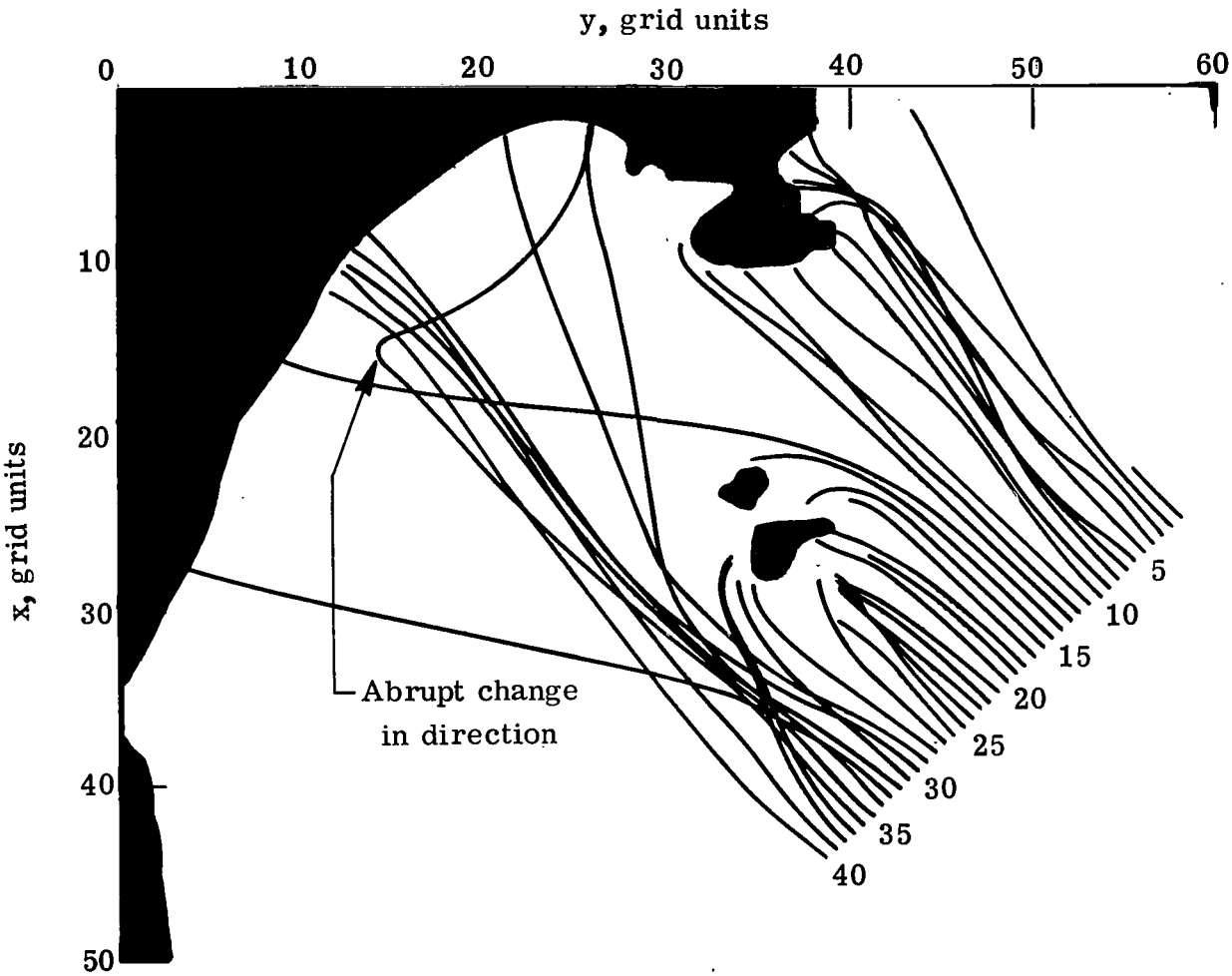

(c) Constrained bicubic interpolation.

Figure 5.- Concluded.

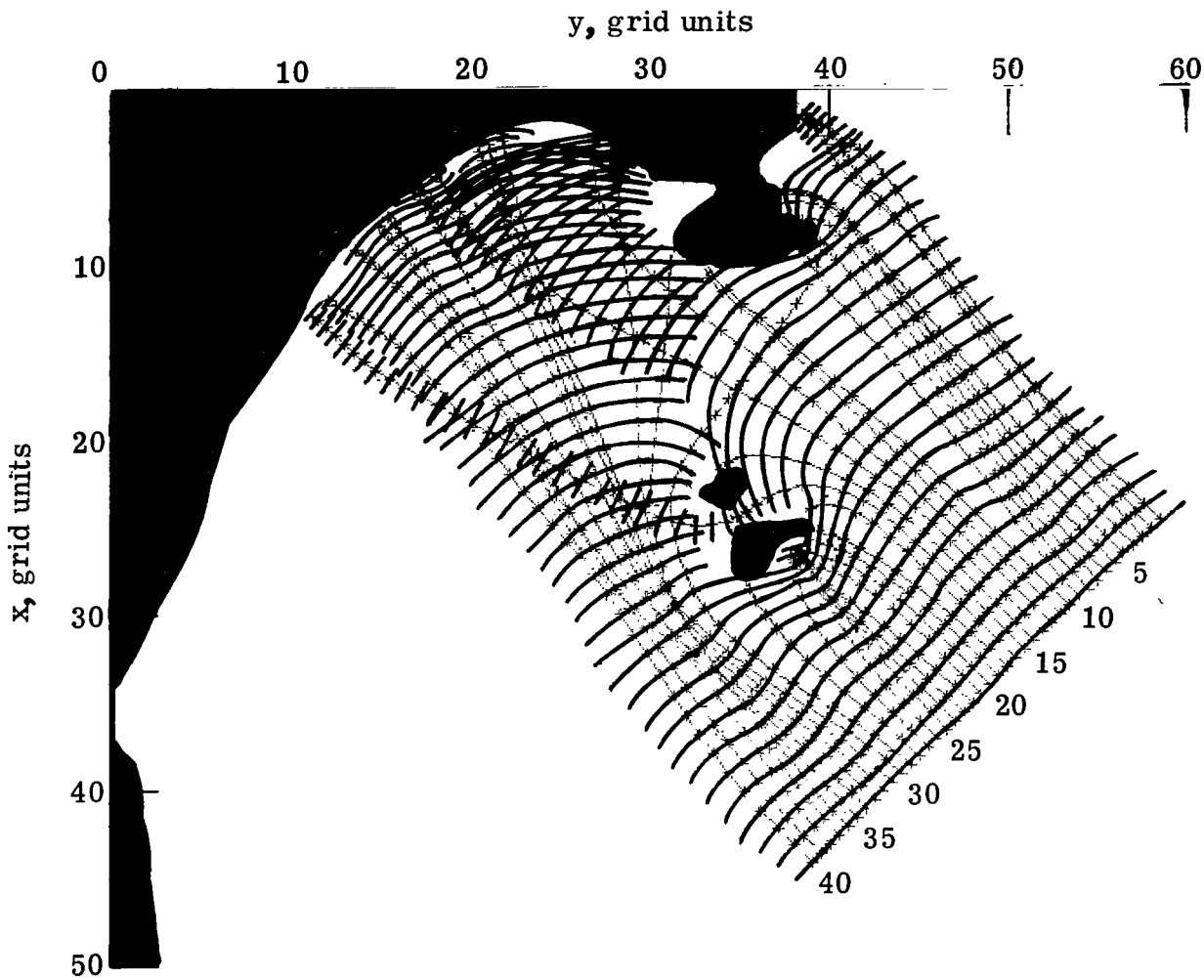

(a) Quadratic least squares.

Figure 6.- Saco Bay wave-crest patterns for different topography approximation techniques.

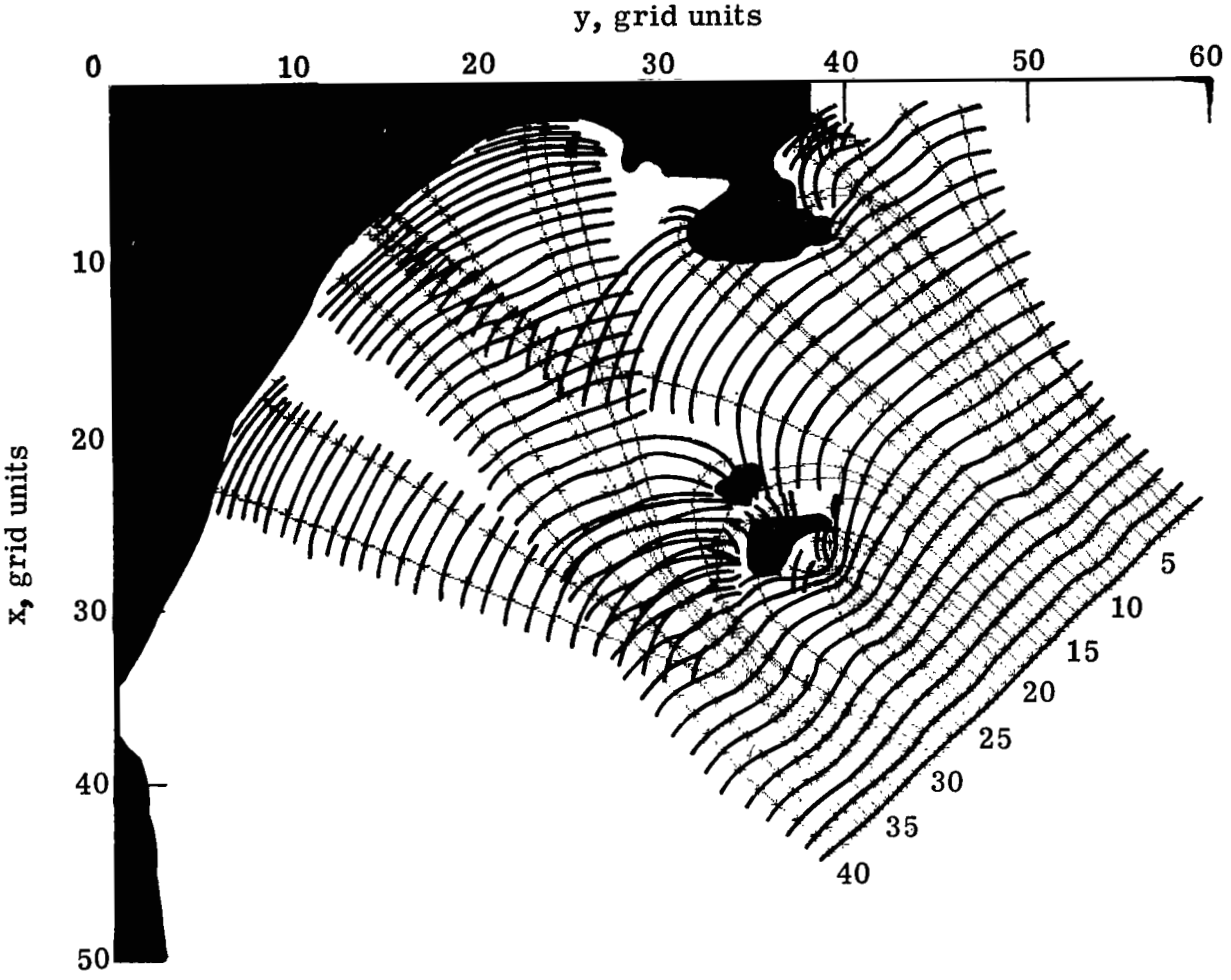

(b) Cubic least squares.

Figure 6.- Continued.

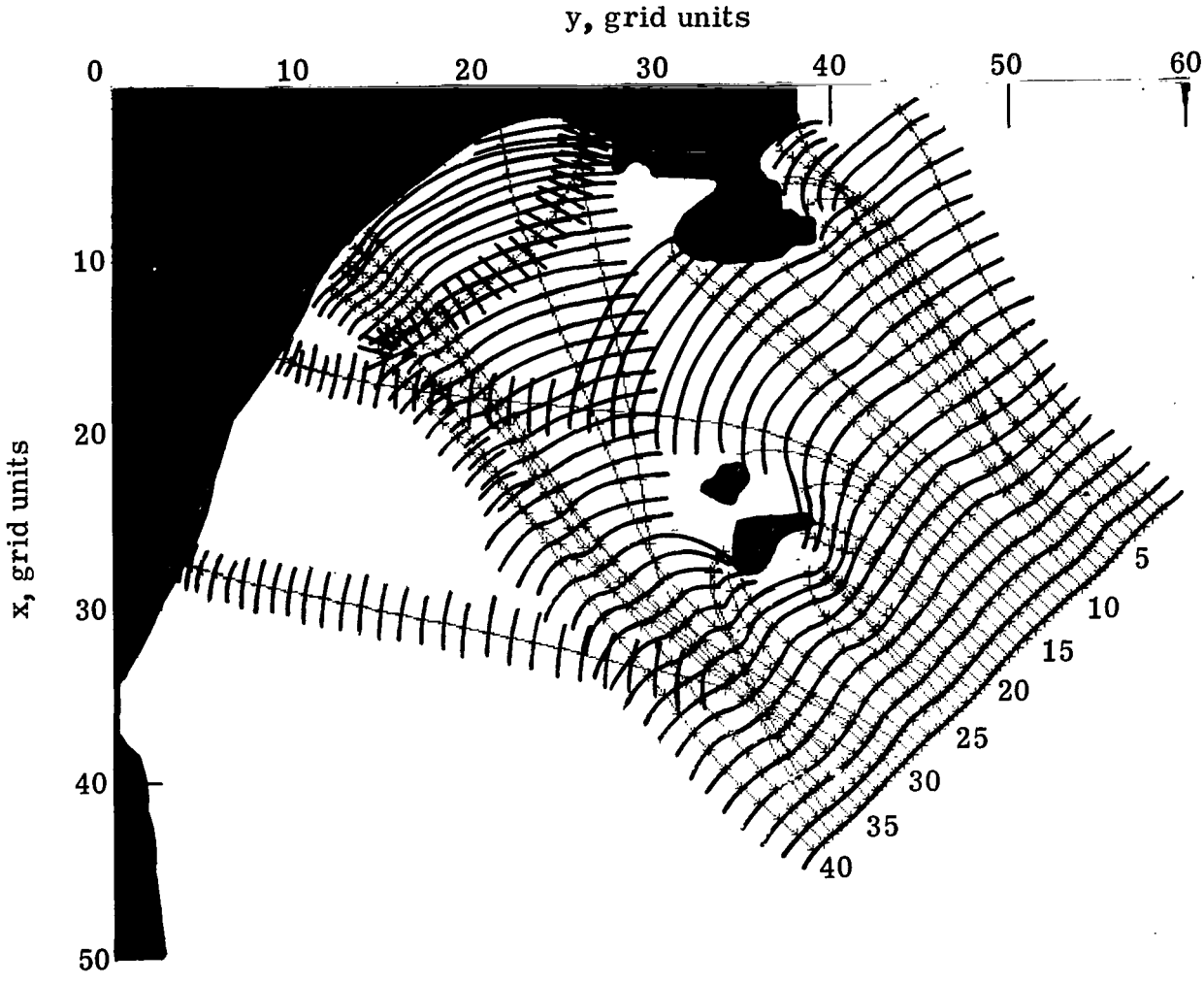

(c) Constrained bicubic interpolation.

Figure 6.- Concluded.

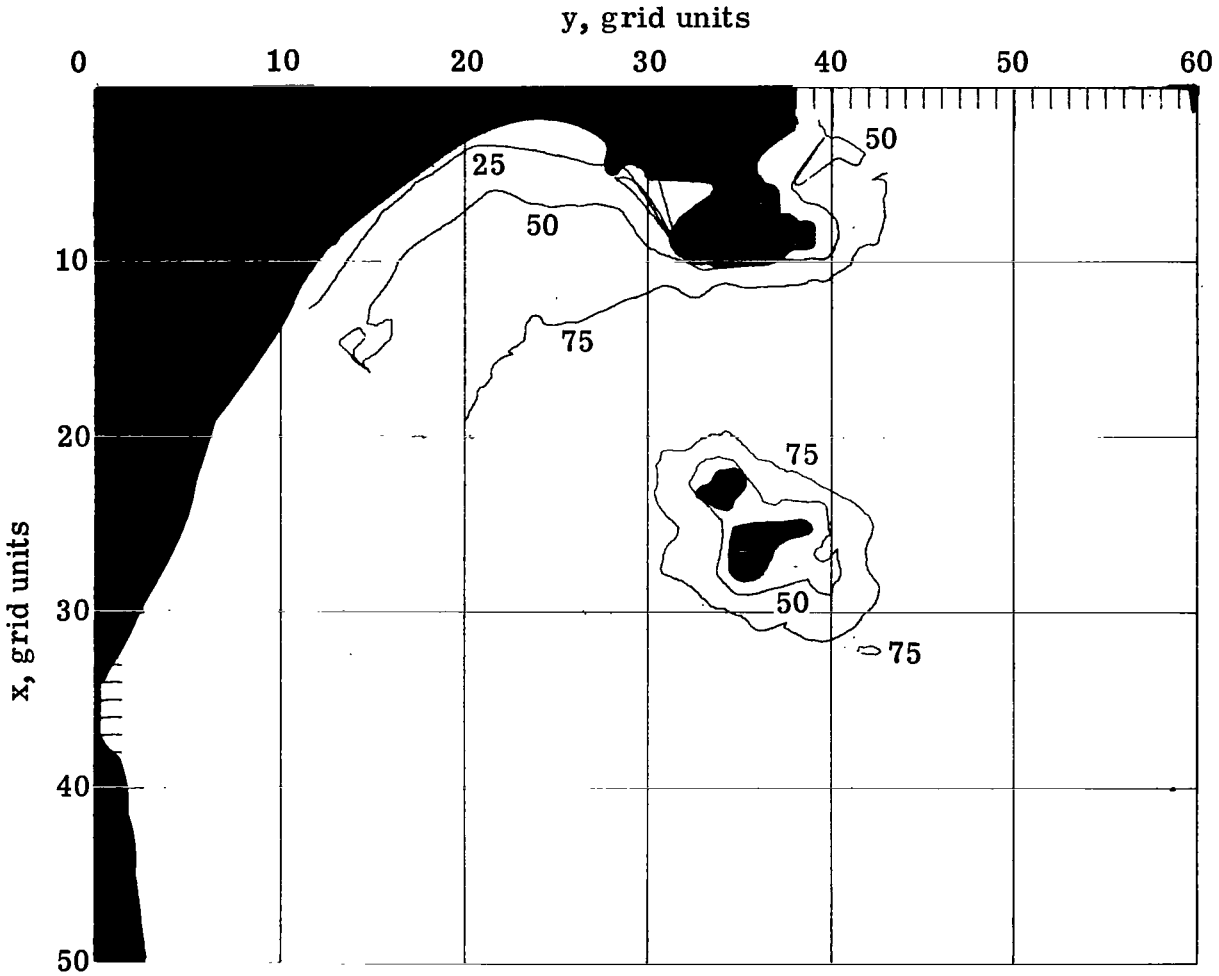

(a) Quadratic least squares.

Figure 7.- Contours of computed wavelength λ at levels of 25, 50, and 75 meters. λ_o = 100 m.

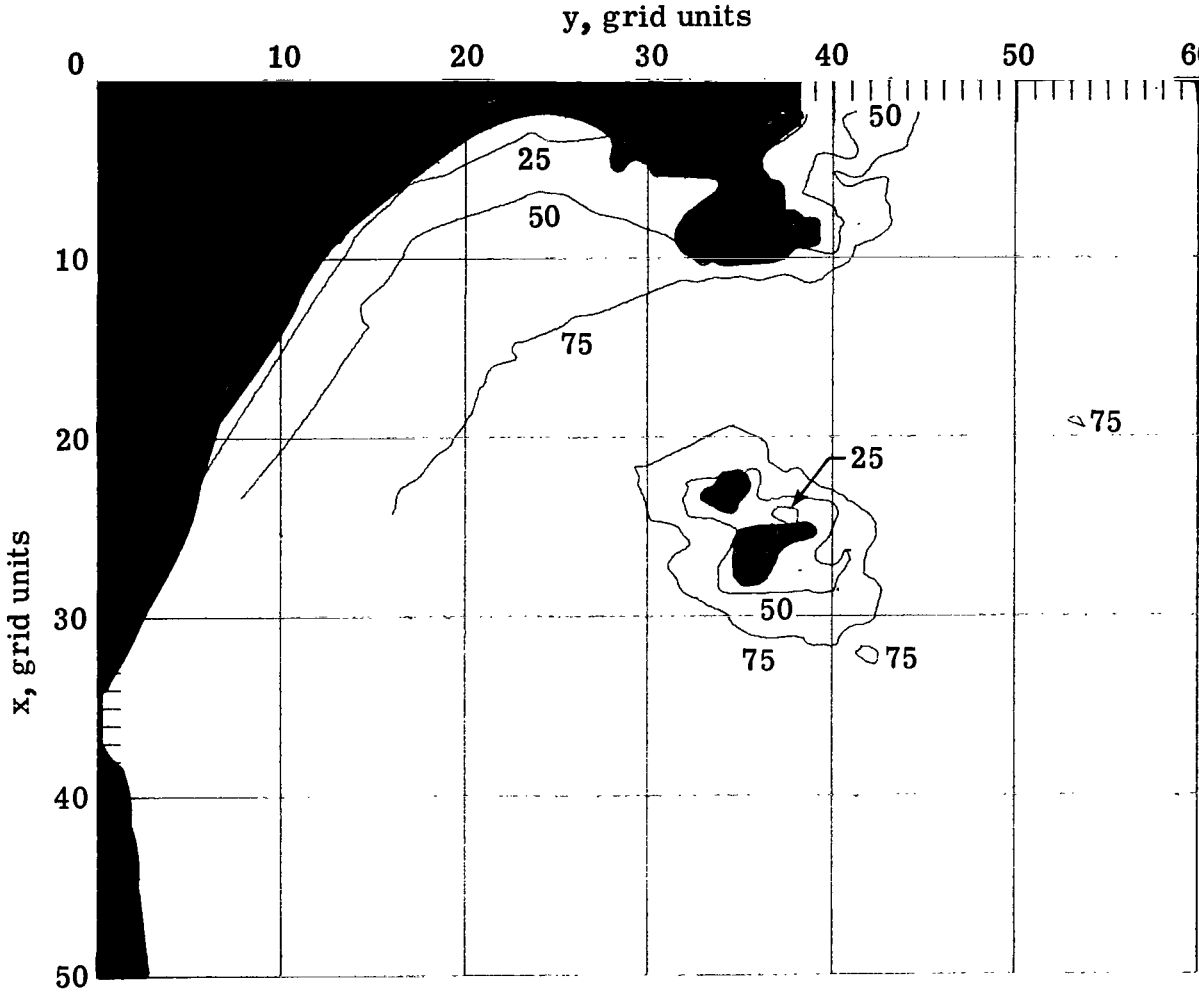

(b) Cubic least squares.

Figure 7.- Continued.

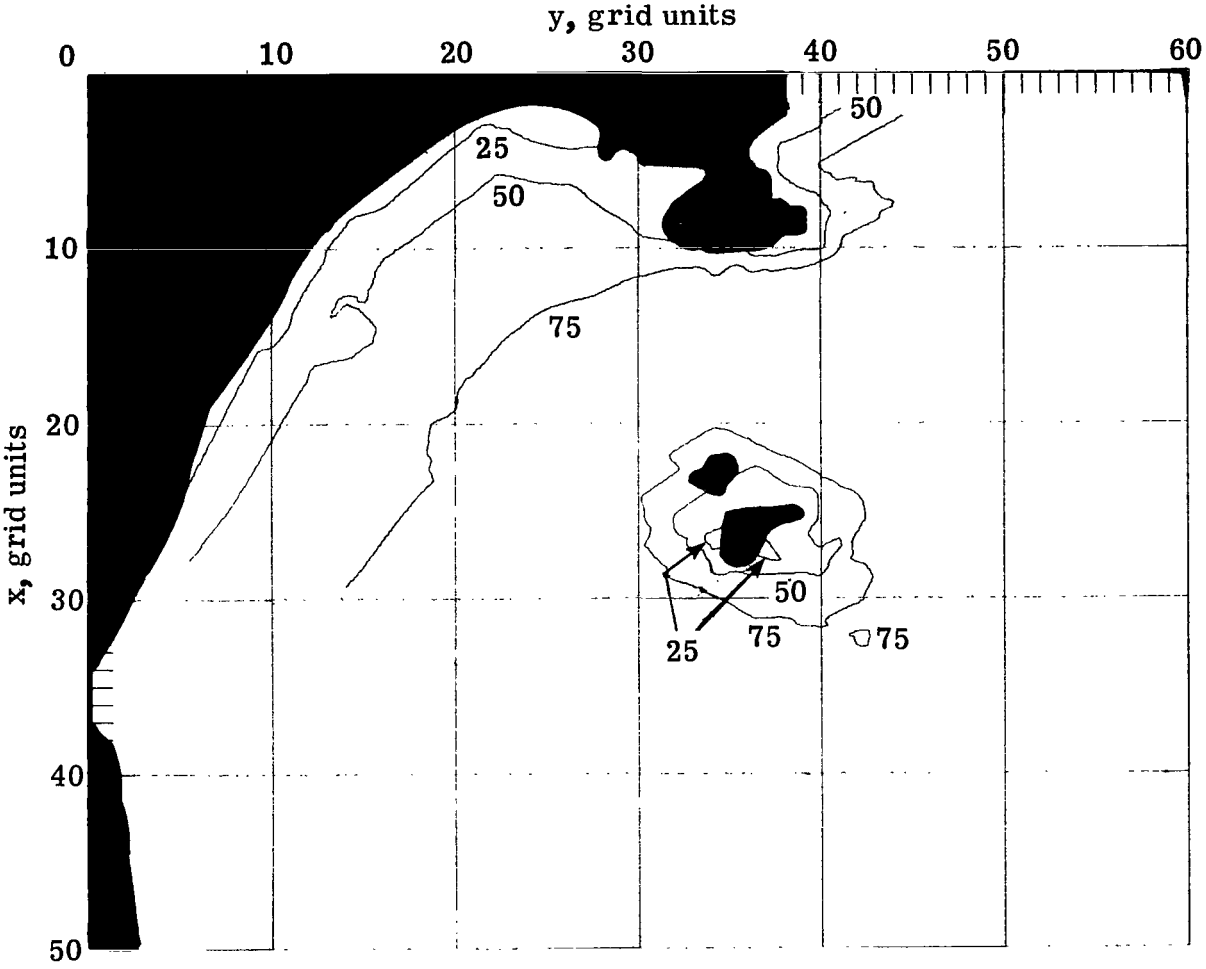

(c) Constrained bicubic interpolation.

Figure 7.- Concluded.

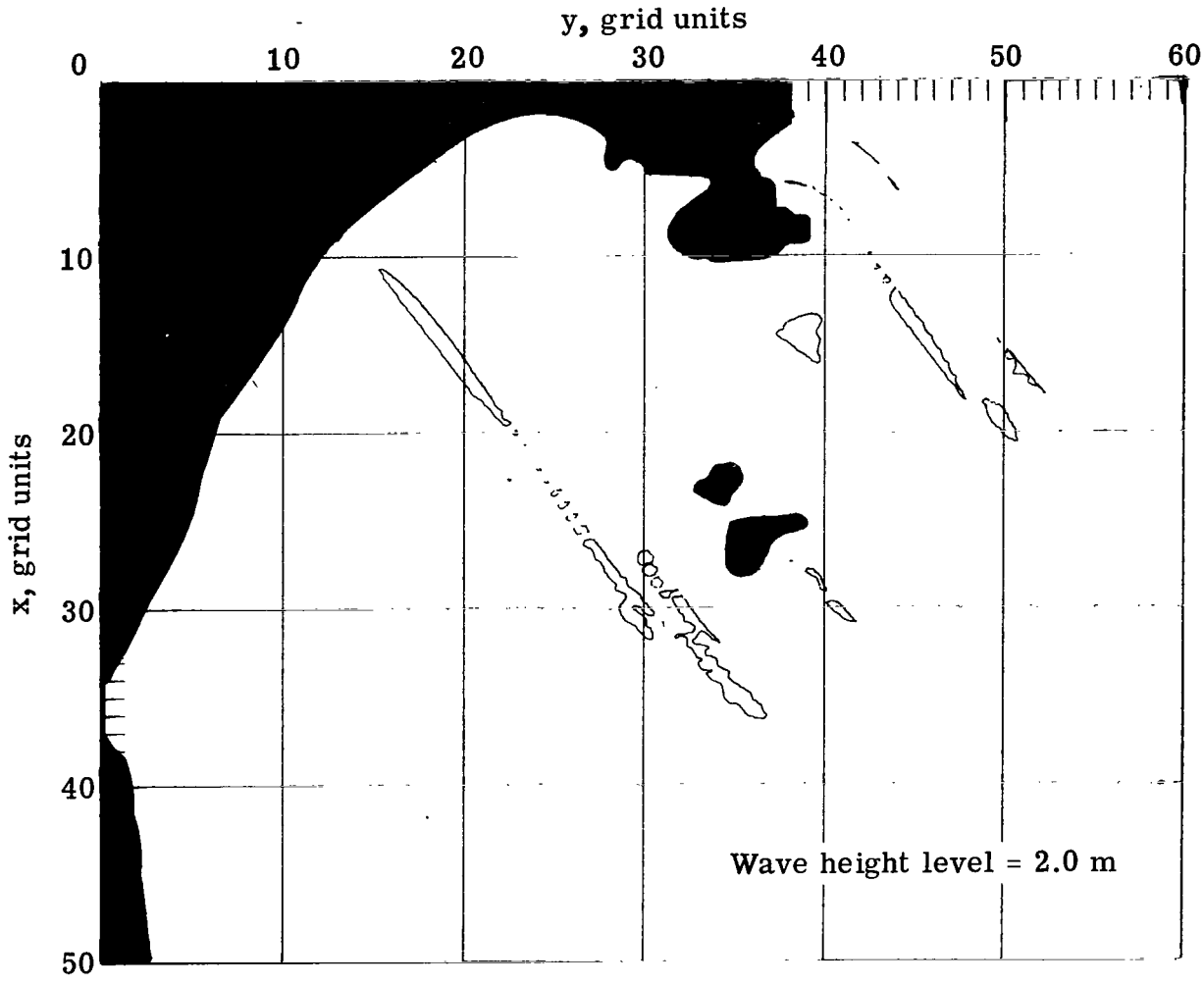

(a) Quadratic least squares.

Figure 8.- Contours of computed wave height H at 2.0-meter level.
H_o = 1.22 m.

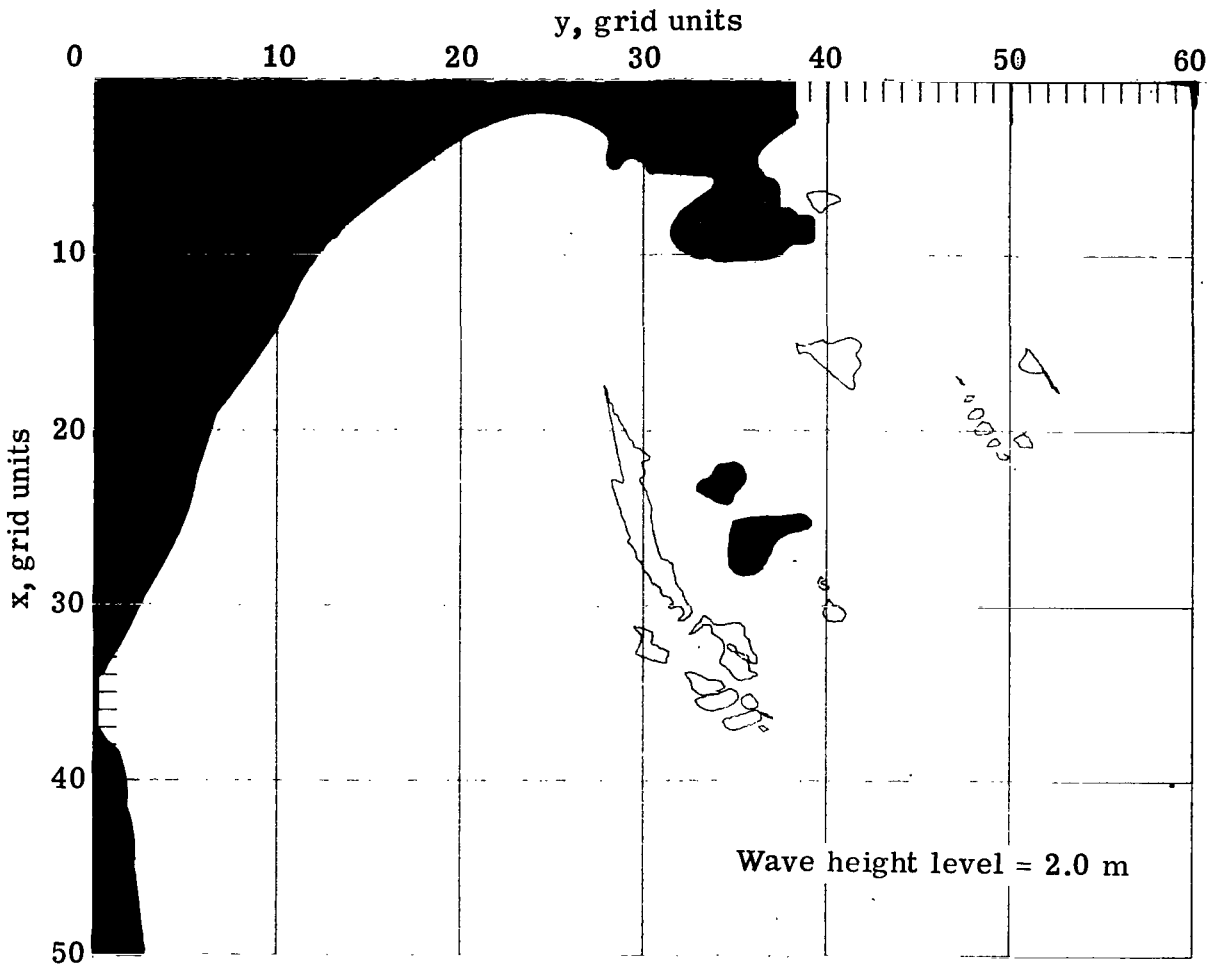

(b) Cubic least squares.

Figure 8.- Continued.

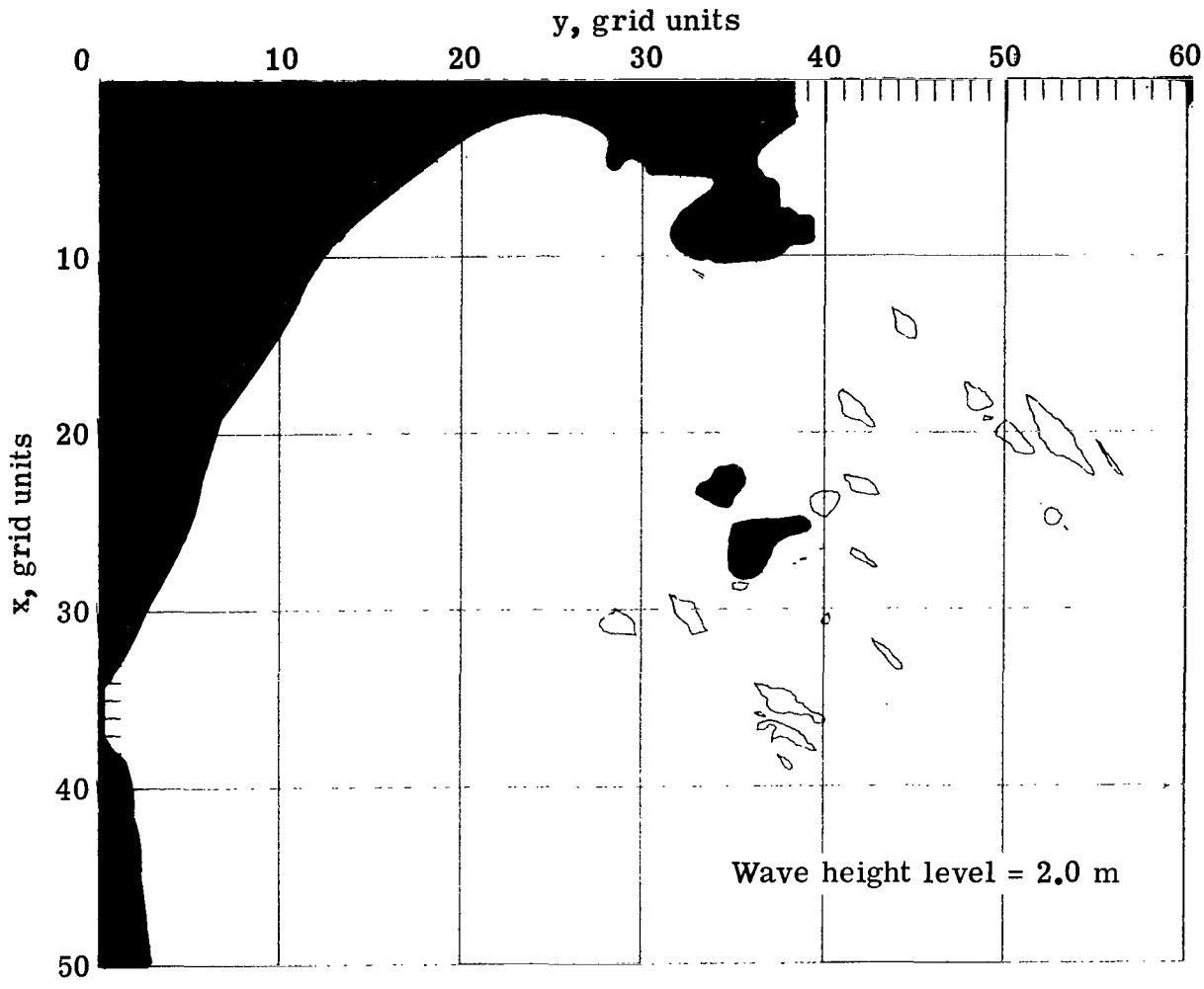

(c) Constrained bicubic interpolation.

Figure 8.- Concluded.

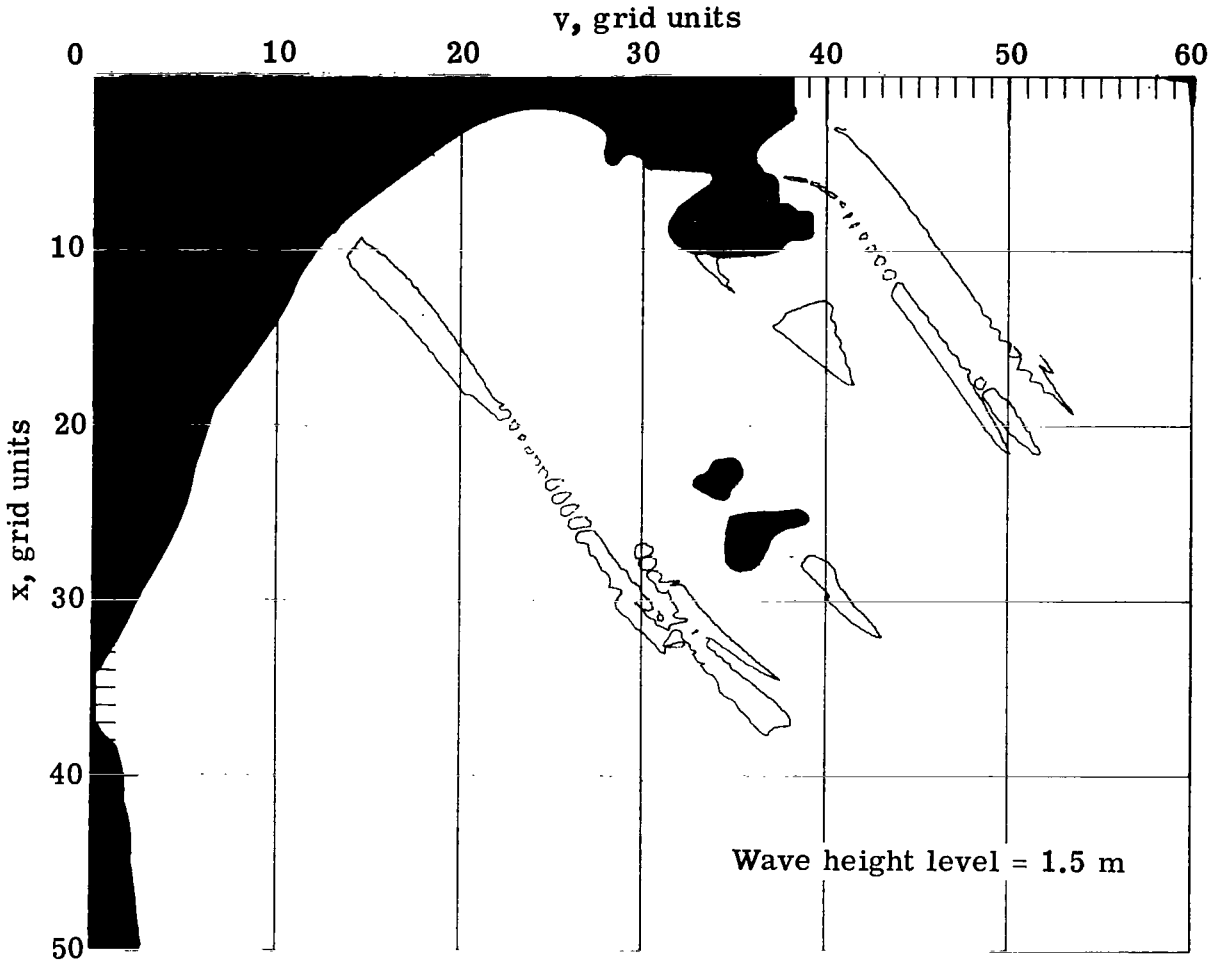

(a) Quadratic least squares.

Figure 9.- Contours of computed wave height H at 1.5-meter level.
H_o = 1.22 m.

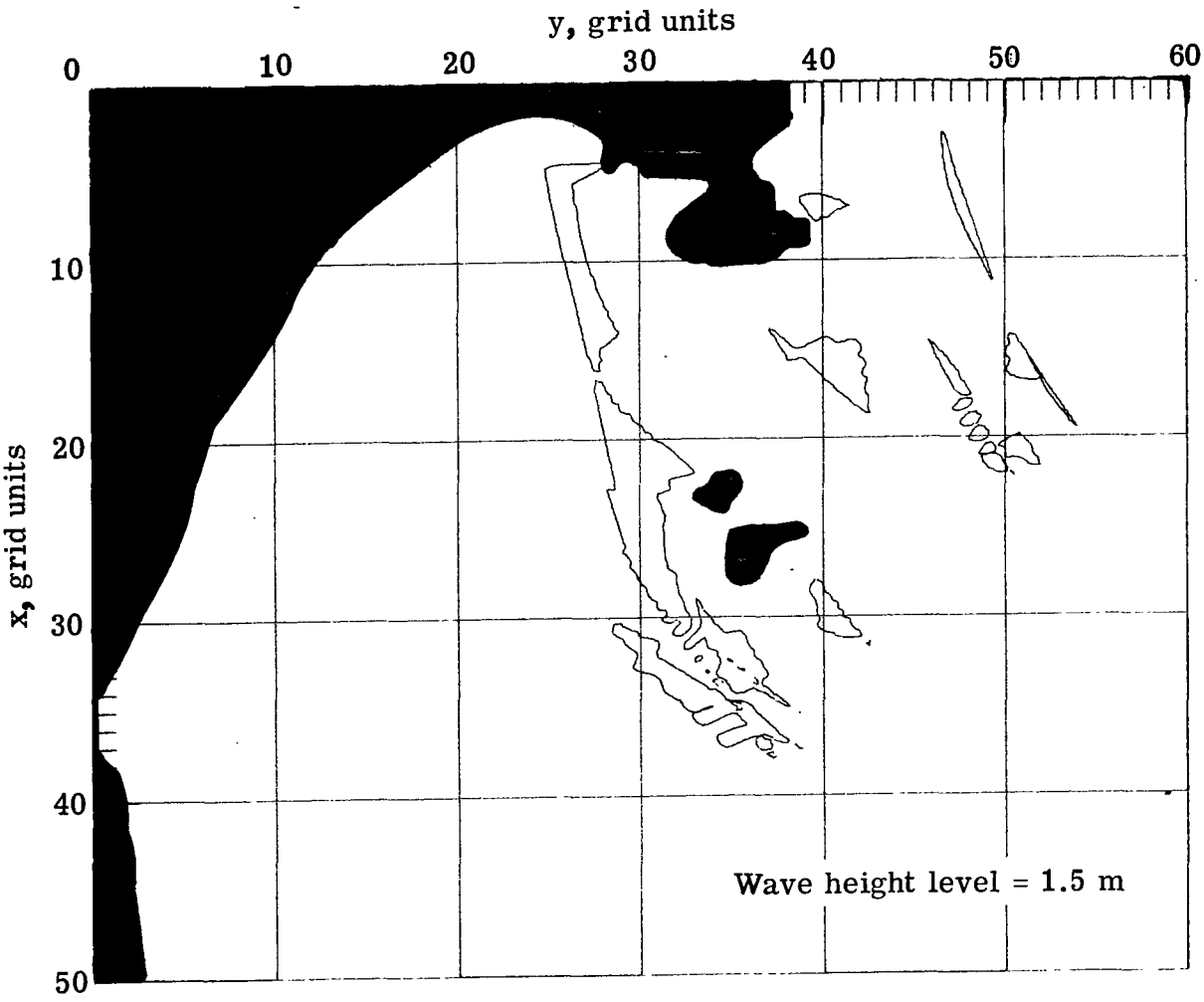

(b) Cubic least squares.

Figure 9.- Continued.

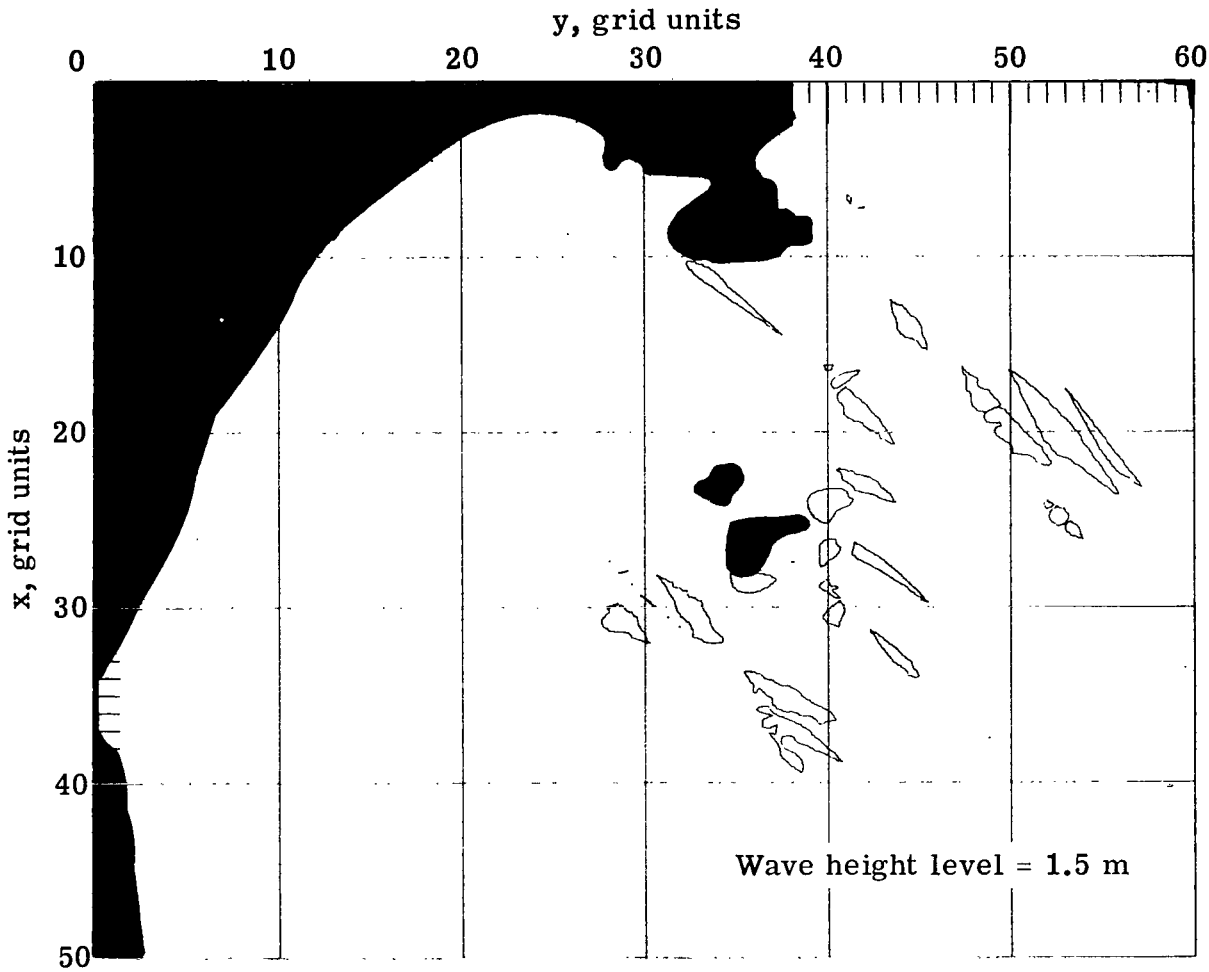

(c) Constrained bicubic interpolation.

Figure 9.- Concluded.

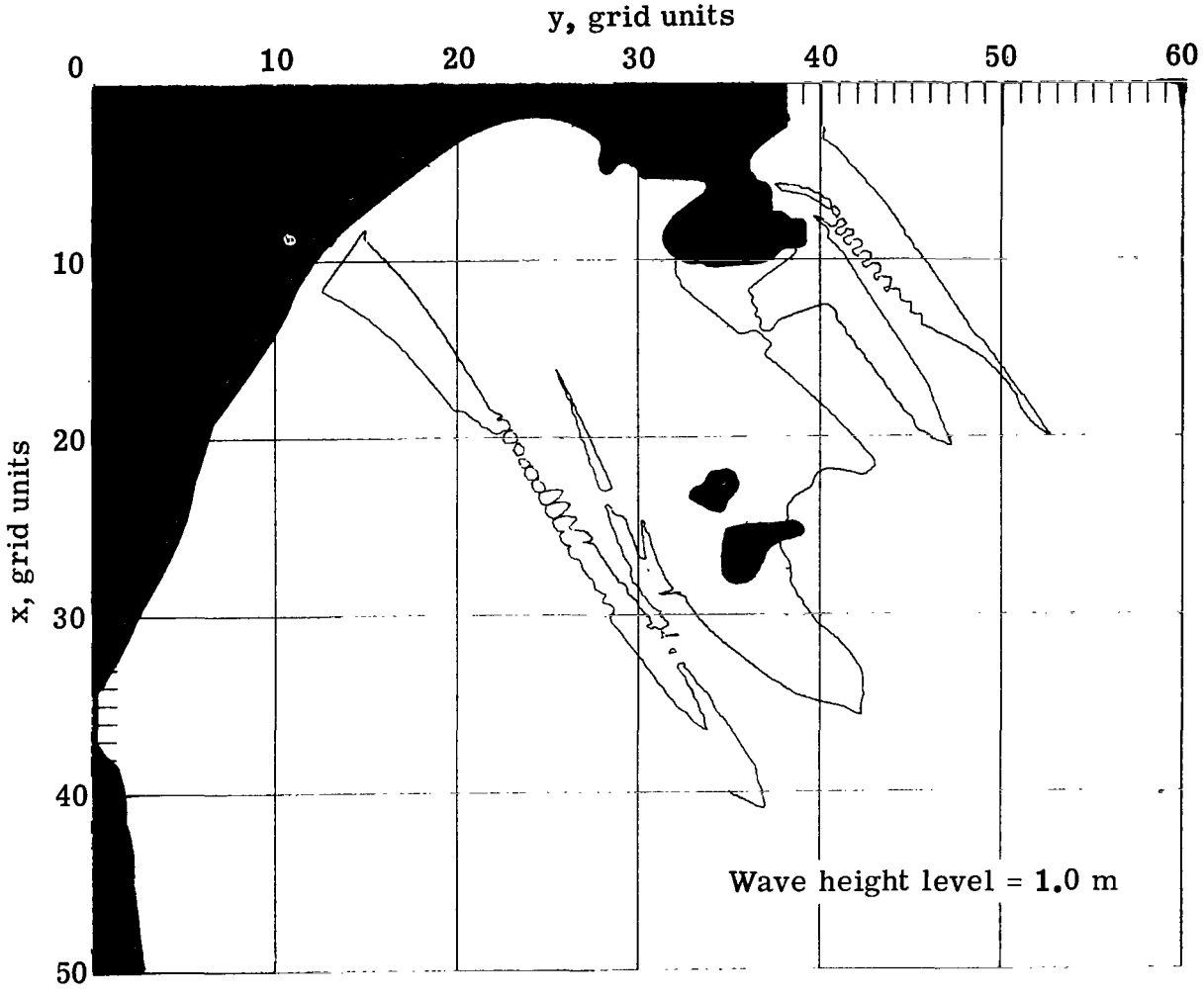

(a) Quadratic least squares.

Figure 10.- Contours of computed wave height H at 1.0-meter level.
H_o = 1.22 m.

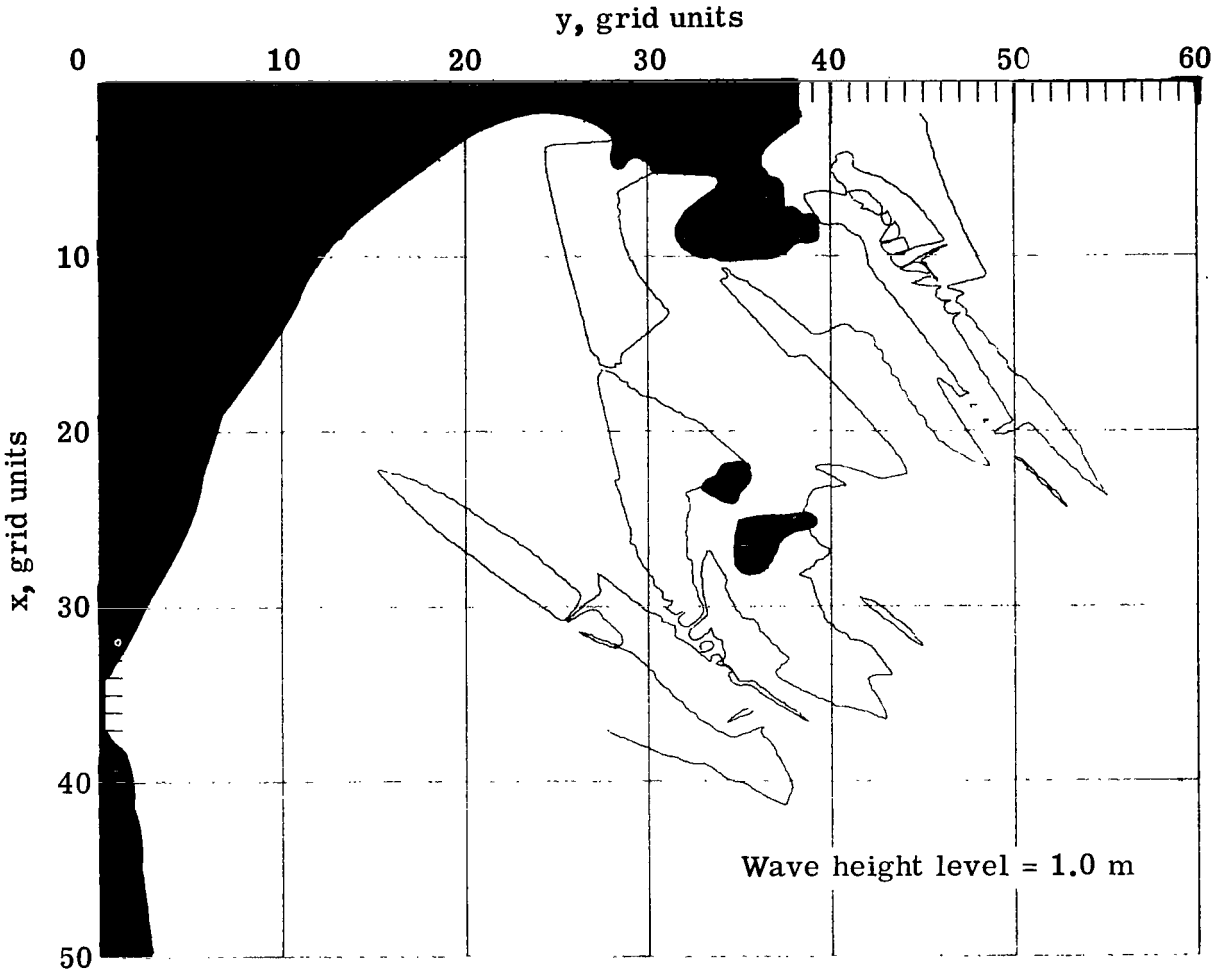

(b) Cubic least squares.

Figure 10.- Continued.

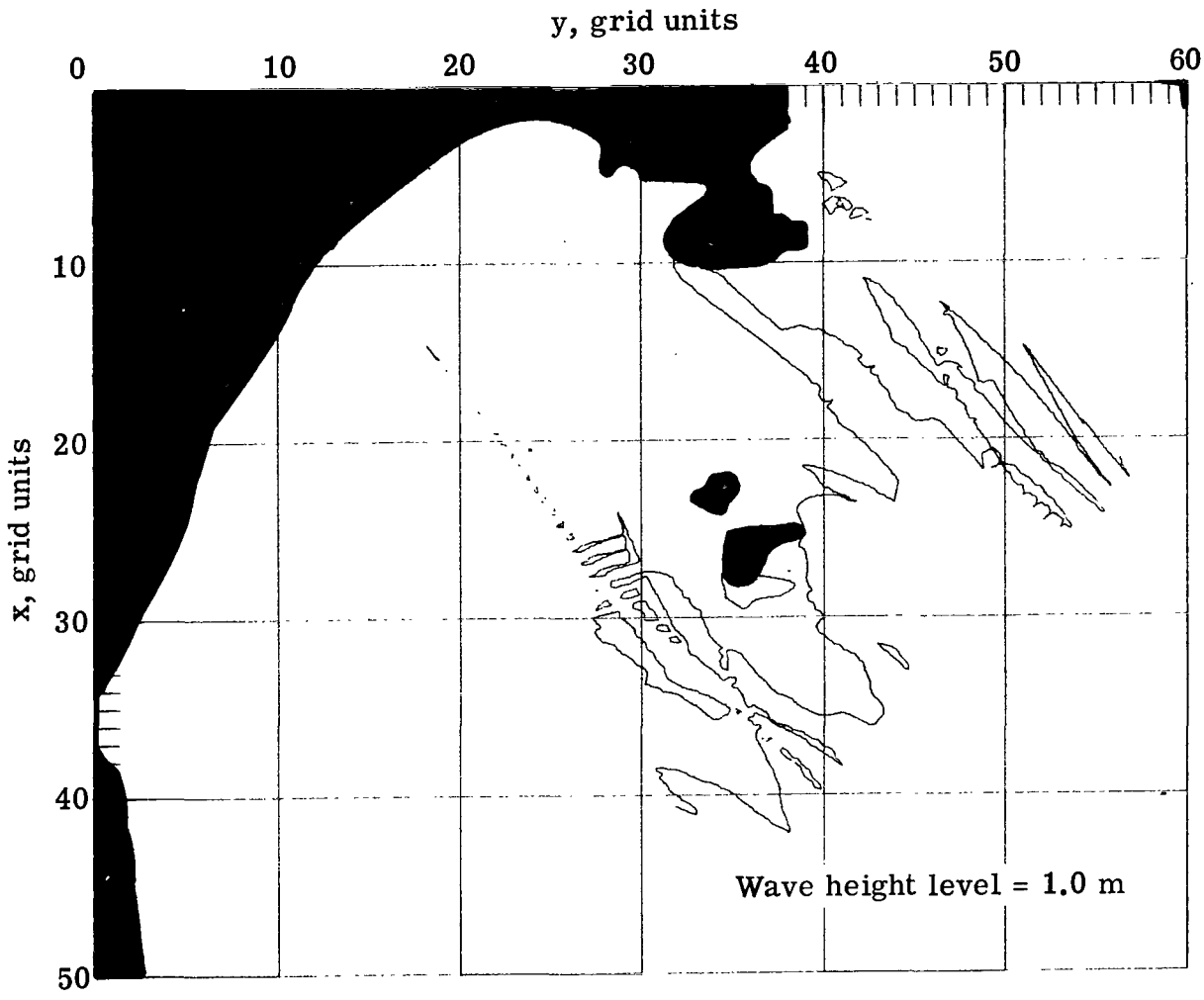

(c) Constrained bicubic interpolation.

Figure 10.- Concluded.

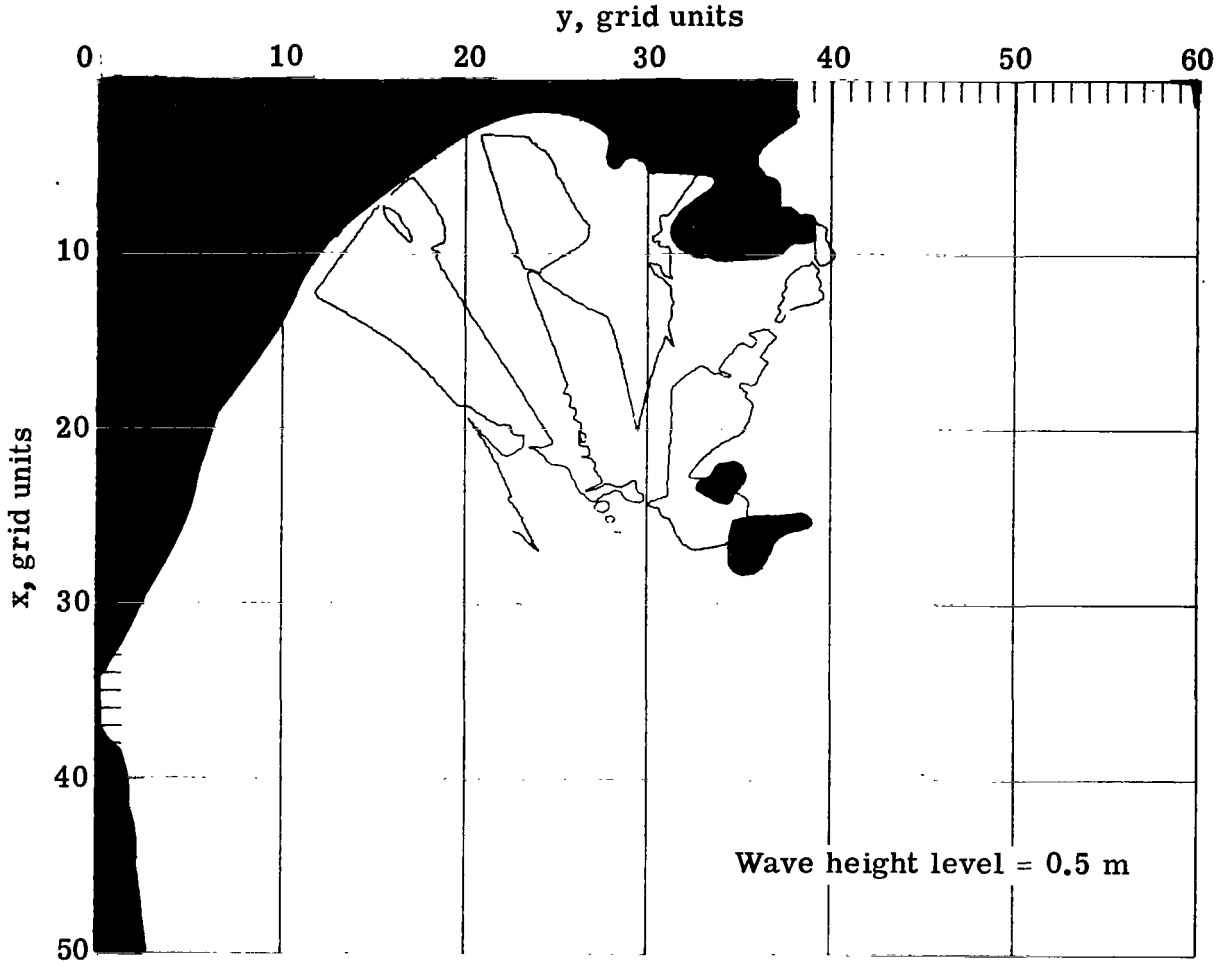

(a) Quadratic least squares.

Figure 11.- Contours of computed wave height H at 0.5-meter level.
H_o = 1.22 m.

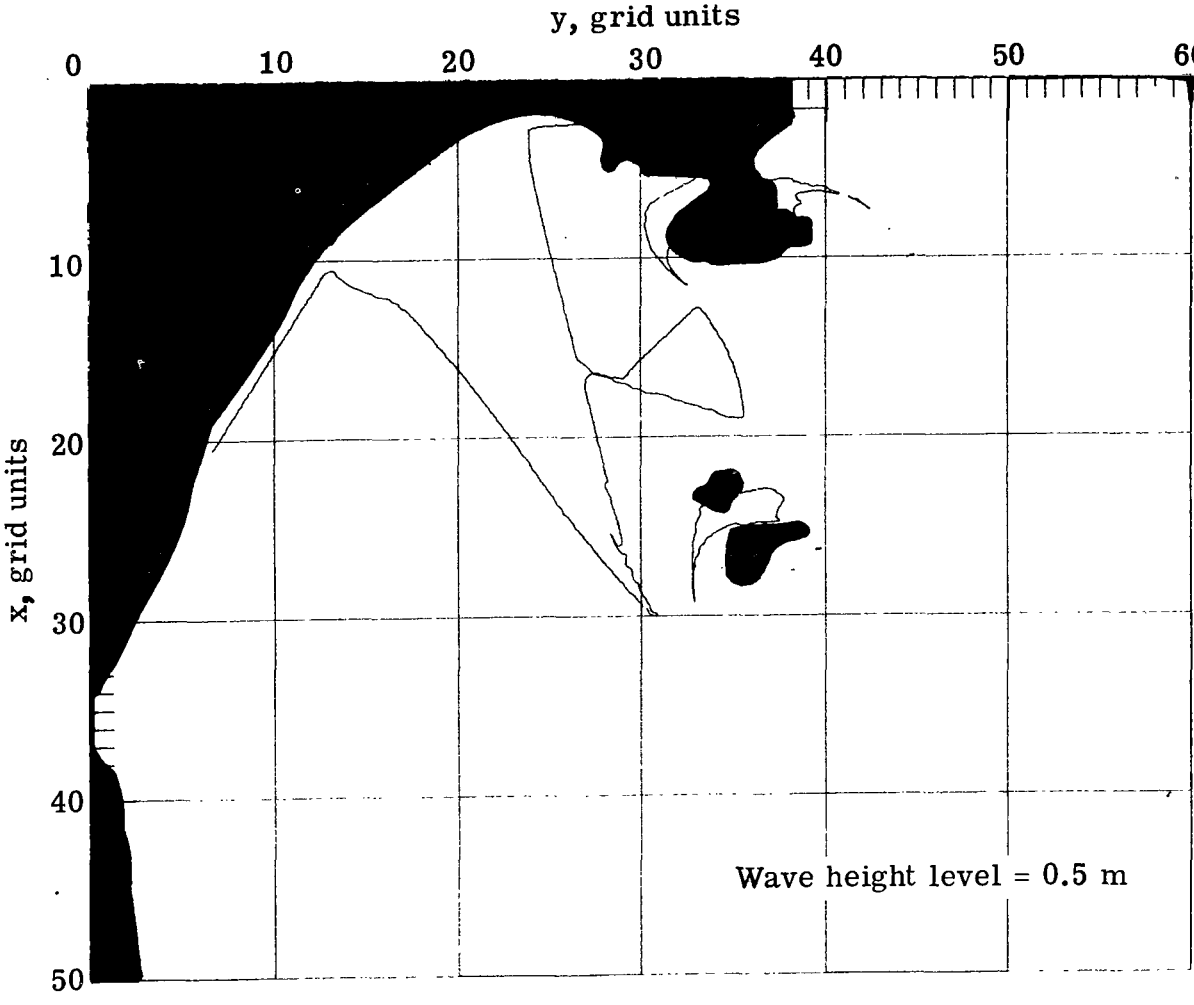

(b) Cubic least squares.

Figure 11.- Continued.

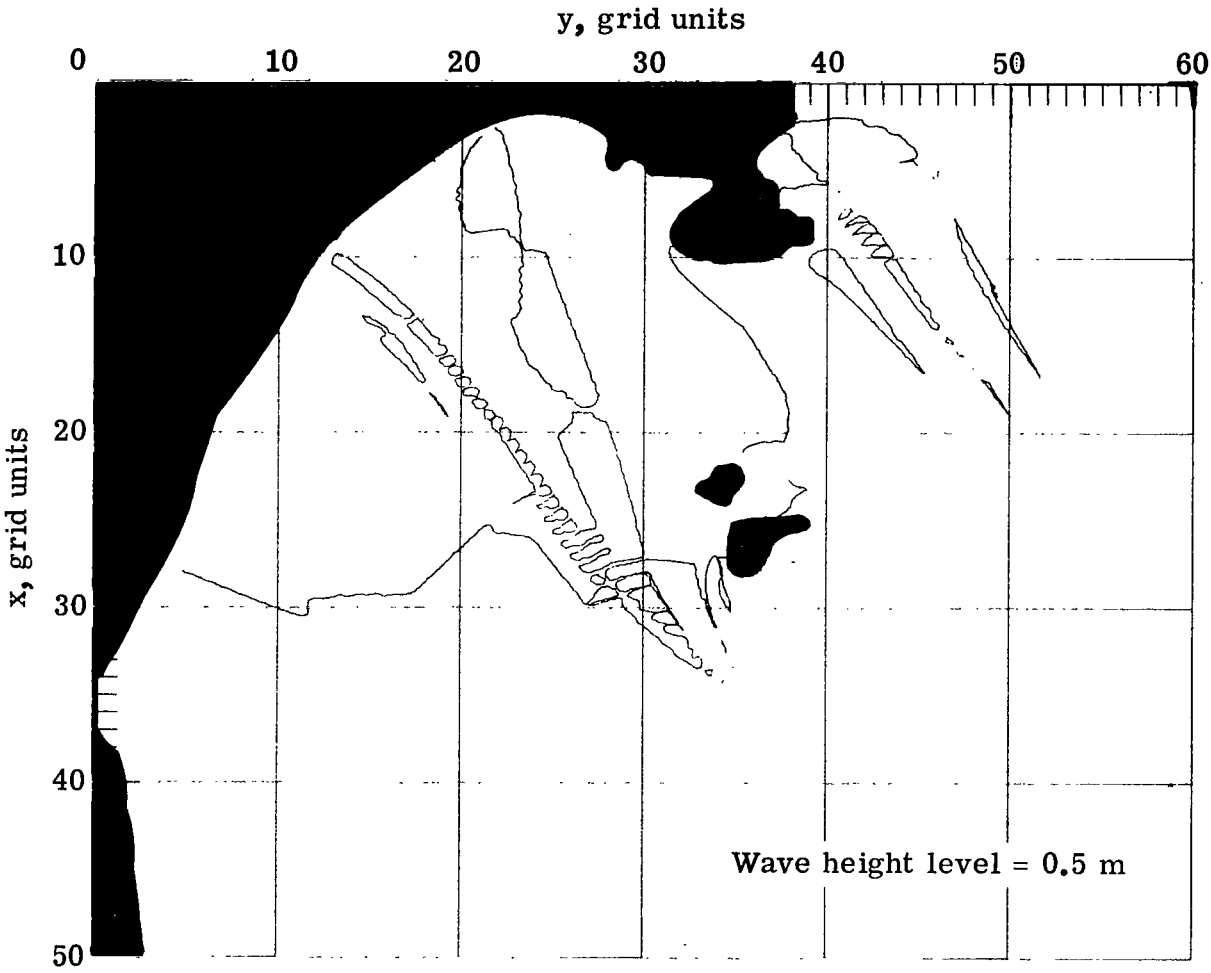

(c) Constrained bicubic interpolation.

Figure 11.- Concluded.

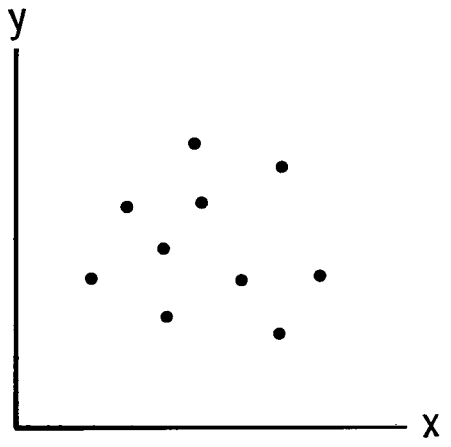

(a) A set of input data points.

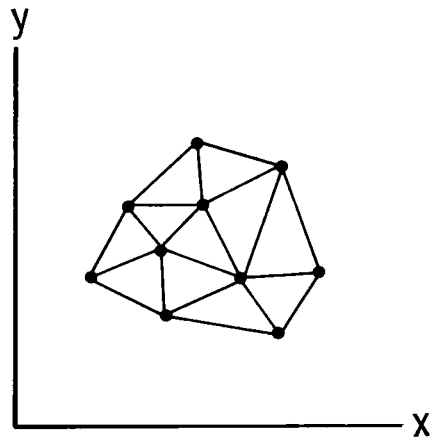

(b) A convex region composed of triangles.

Figure 12.- Contouring process.

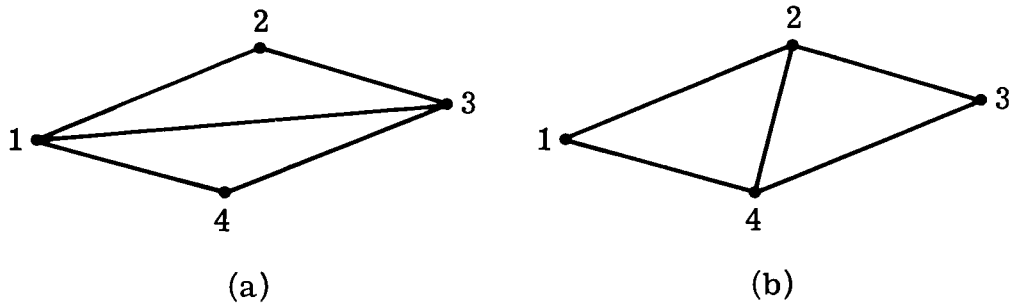

Figure 13.- Two choices for arranging triangles for four data points.

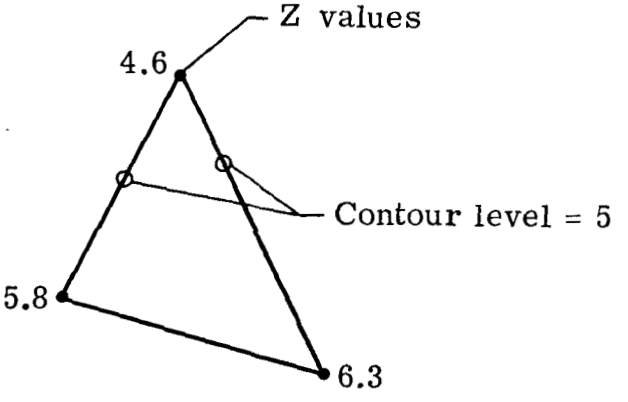

Figure 14.- A triangle with linearly interpolated contour points.

NASA-Langley, 1975 L-10320

"The aeronautical and space activities of the United States shall be conducted so as to contribute . . . to the expansion of human knowledge of phenomena in the atmosphere and space. The Administration shall provide for the widest practicable and appropriate dissemination of information concerning its activities and the results thereof."

—NATIONAL AERONAUTICS AND SPACE ACT OF 1958

NASA SCIENTIFIC AND TECHNICAL PUBLICATIONS

TECHNICAL REPORTS: Scientific and technical information considered important, complete, and a lasting contribution to existing knowledge.

TECHNICAL NOTES: Information less broad in scope but nevertheless of importance as a contribution to existing knowledge.

TECHNICAL MEMORANDUMS: Information receiving limited distribution because of preliminary data, security classification, or other reasons. Also includes conference proceedings with either limited or unlimited distribution.

CONTRACTOR REPORTS: Scientific and technical information generated under a NASA contract or grant and considered an important contribution to existing knowledge.

TECHNICAL TRANSLATIONS: Information published in a foreign language considered to merit NASA distribution in English.

SPECIAL PUBLICATIONS: Information derived from or of value to NASA activities. Publications include final reports of major projects, monographs, data compilations, handbooks, sourcebooks, and special bibliographies.

TECHNOLOGY UTILIZATION PUBLICATIONS: Information on technology used by NASA that may be of particular interest in commercial and other non-aerospace applications. Publications include Tech Briefs, Technology Utilization Reports and Technology Surveys.

Details on the availability of these publications may be obtained from:

SCIENTIFIC AND TECHNICAL INFORMATION OFFICE

NATIONAL AERONAUTICS AND SPACE ADMINISTRATION

Washington, D.C. 20546